

# Chapter 4

## LASER-INDUCED CHANGES IN VISUAL PERFORMANCE: IMMEDIATE AND LONG-TERM CONSEQUENCES IN AN ANIMAL MODEL

DAVID O. ROBBINS, PhD,\* AND HARRY ZWICK, PhD†

---

INTRODUCTION

METHODS

Subjects and Apparatus

Discrimination Task

Laser Exposures

Data Analysis

RESULTS

DISCUSSION

SUMMARY

\*Department of Psychology, Ohio Wesleyan University, 61 South Sandusky Street, Delaware, Ohio 43015

†US Army Medical Research Detachment, Walter Reed Army Institute of Research, 3201 Sidney Brooks, Brooks Air Force Base, Texas 78235-5138; Deceased

## INTRODUCTION

The nature of the eye's highly absorptive pigments, as well as its optical and mechanical properties, makes this organ a prime candidate for light-induced damage. Damage to the central region of the eye, the fovea, is particularly important in any clinical or applied analysis because this retinal region is responsible for fine spatial resolution and color vision. The retinal layers in this region are thin and form the foveal "pit," where the density of cone photoreceptors is the highest. The distribution of cone photoreceptors containing visual pigments with different absorption spectra is not uniform within this area.<sup>1,2</sup> Hence, predicting the amount of loss in visual functioning resulting from tissue damage in this area is a complex fusion of many considerations. The specific characteristics of laser exposure are important as are considerations of the exposure site, including its absorption characteristics and plasticity. The nature of the exposure site can also be influenced by the age and general health of the patient, as well as the patient's prior exposure to light.

As reported elsewhere in this book, retinal damage thresholds from laser irradiation traditionally have relied on fundoscopic and/or histological evidence from single or multiple exposures presented to anesthetized animals over a very limited time period. These studies have provided clear evidence for the presence and location of morphological insult that result from relatively intense retinal exposures, and the additional impact that multiple pulses presented in the same general retinal region have on the shape and degree of retinal insult.<sup>3,4</sup> Using different exposure conditions, various damage mechanisms have been proposed to explain variations in the susceptibility and severity of the elicited damage. Generally, on the one hand, a thermal model has been attributed to those changes resulting from relatively long-duration, low-energy exposures to long-wavelength coherent light. On the other hand, mechanical damage mechanisms have typically been associated with extremely high-energy, short-duration (Q-switched) pulses. Less frequently cited are the more subtle changes associated with repeated low-energy exposures at power levels well below those where either thermal or mechanical disruptions would be predicted. In these cases, it has been proposed that laser irradiation might produce photoreceptor and/or photopigment damage that ultimately could affect the receptor transduction process and even the viability of the receptor cell itself.<sup>5-7</sup> It might be expected that functional changes associated with these more subtle retinal alterations would be a more sensitive measure of the adverse effects of low-level laser irradiation because these types of

subtle physical changes in retinal morphology and/or photochemistry would be extremely difficult to detect in an intact retina.

As morphological techniques for detecting minimal retinal alterations have been refined, the energy densities necessary to produce observable retinal lesions have themselves decreased. Associated with these refined techniques and combined with minimal exposure conditions have been a shift in the site of primary anatomical alteration from the corneal and pigment epithelial layers to the outer segments of the photoreceptors.<sup>8-10</sup> Although the site of morphological disruption observed is the location where the initial transduction of light energy to electrochemical energy occurs, it is also important to consider the behavioral (functional) consequences of any induced physical change. Changes in the functional capacities of the retina have specific legal, medical, and, ultimately, practical consequences, especially considering how much human behavior is based on accurate visual assessments of the physical world.

Developing a model for predicting the amount of loss in visual performance that results from laser-induced damage to the retina is a complex, but obviously important, part of any laser safety program. Clearly, the type and degree of visual deficits depend not only on the specific characteristics of the laser exposure, but also on the amount, location, and severity of retinal dysfunction, as well as on the functional integrity of surrounding retinal regions. Accurately predicting behavioral outcomes may also depend on two other considerations. Exposed individuals often develop other viewing strategies that consciously or unconsciously depend on the use of surrounding unexposed areas within the affected eye and/or shift to the unexposed eye that previously may not have been the individual's dominate eye. It is also possible that regenerative retinal mechanisms and/or brain mechanisms may be activated to override transformation alterations in the eye's opacity to light. Changes in subtle photochemical transduction mechanisms could also influence the electrochemical cascades that initiate neural signals within the retina and beyond.

Obviously, direct human experimentation in this area is impossible, and the study of human laser accident cases lacks precision because dosimetry estimates are necessarily post hoc, and sustained participation from the patients is often difficult to procure. Regardless, human studies have again demonstrated the morphological and functional uniqueness of the fovea.<sup>11,12</sup> Damage to the fovea has been shown to cause rather dramatic deficits in visual acuity consistent with the

morphological and resolution capacities of the surrounding retinal regions. Some recovery in visual acuity is typically seen in patients receiving low-level exposures, suggesting possible retinal and/or brain regeneration mechanisms that might override any initial morphological damage.<sup>13–15</sup> Early explanations of this recovery implied that normal photoreceptors adjacent to the damaged site might passively repopulate the damaged fovea and restore some of the original foveal receptor matrix density.<sup>8</sup>

In patients who have experienced more intense exposures, no recovery is evident.<sup>9</sup> In such cases, secondary damage mechanisms, such as retinal scar formation and nerve fiber layer (NFL) damage, have been induced. This type of damage may physically alter photoreceptor density in the fovea by traction induced by scar tissue. Damage to the NFL in the papillomacular bundle could also impact neural communication to the brain.<sup>16</sup> The nature and limiting factors regulating the regeneration of damaged neurons were first described by Ramon and Cajal<sup>17</sup> and suggested that damaged neurons are capable of only abortive sprouting and little functional recovery. One of the major barriers to regeneration is the formation of glial scarring. More recent research has shown that the previously considered sterile dystrophic end bulbs can return to active growth states<sup>18</sup> and remain active for days after injury.<sup>19</sup> Interestingly, the ability of axons to regenerate depends not only on the maturity of astrocytes and the astroglial reaction to injury, but also on the type of neuron. Sensory neurons, especially retinal ganglion cells, appear capable of eliciting the most growth, although all evidence to date suggests that these cells eventually succumb to the reactive glial response that inhibits such growth.<sup>20,21</sup>

Experimental studies using animals to determine the minimal visible lesion threshold energy provide excellent dosimetry, because exposure levels can be measured during the experimental operations. However, these investigations typically employed small spot exposures involving large areas outside of the fovea to minimize variability in threshold determinations. Foveal photoreceptor architecture and photopigment and pigment epithelium layer absorption properties within the fovea differ dramatically from one spot to another.<sup>22</sup> The majority of these studies also excluded any direct assessment of the actual visual loss and assumed instead that these losses could be predicted based on traditional psychophysical investigations of the sensitivity of various retinal regions in the intact eye.

A number of lines of evidence might lead one to conclude that the loss of foveal function would be catastrophic. One would expect the greatest loss of

photoreceptors, as well as the greatest loss in acuity and color vision. Recent laser accident studies and animal behavioral studies assessing the impact that acute foveal injury has on visual acuity support this notion, but also suggest some degree of neural plasticity.<sup>23</sup> Under certain exposure conditions, foveal exposures that seriously damage photoreceptors produce only minimal scar, traction, and retinal NFL damage. In these cases, animals may fully recover their initial loss in visual acuity.<sup>24</sup> Proposed mechanisms for this recovery have been based in part on the repopulation of lost foveal photoreceptors that has been observed histologically.<sup>8</sup> It has also been based in part on more active mechanisms that might involve efferent cortical retinal modulation<sup>16,24</sup> and neural plasticity in higher centers within the visual pathway.<sup>25</sup>

In the earlier days of what was then called the Laser Safety Program—in collaboration with researchers at Frankford Arsenal in Philadelphia and the Armed Forces Institute of Pathology in Washington, DC—we developed a reliable behavioral task to measure visual acuity losses in animals that, under anesthesia, had been previously exposed to multiple spots of continuous wave (CW) laser light. These animals demonstrated variable degrees of loss in visual acuity and wavelength sensitivity, depending on the location and severity of the retinal damage. Unfortunately, the training technique that we used to measure visual acuity in these animals took a considerable amount of time to complete and did not begin until after the animals were exposed. As a consequence, the initial measures of visual loss did not begin until months after the exposures had been made. Pathological identification of the lesion sites in these animals was further delayed by behavior analysis and, in some cases, was not completed until years later. During this time, one could expect considerable changes in both retinal pathology and function.

Given our success in identifying acuity losses to even minor retinal changes, we changed our approach and developed a method to expose awake, task-oriented animals without the use of anesthesia.<sup>26</sup> This method required the animal to look through a pinhole and fixate on a specific location on a small viewing screen that allowed us to accurately place exposures in and around the fovea. Because the animal was awake during these exposures, we were able to complete behavioral analysis of visual acuity changes during and immediately after each exposure. The initial CW laser exposures that we made were relatively long (>100 ms) and large in diameter (>100  $\mu\text{m}$ ). To evaluate the effectiveness of our procedure, we conducted a number of experiments examining the relationship between spot size and exposure duration on the magnitude and

duration of the induced visual loss. For foveal exposures, the laser was positioned so that it became coaxial with the critical feature in the visual image that the animal was required to discern. Once validity and reliability of methodology were established for cases of flash blindness, our basic empirical question shifted first to define the transitional zone between transient and permanent changes in visual acuity for

various types of CW and Q-switched exposures, then to contrast the impact of foveal versus parafoveal exposures. It was followed by the impact of cumulative exposures over a period of days or weeks at or below the median effective dose ( $ED_{50}$ ) level, and it finally examined the plasticity of retinal functioning due to any regenerative processes occurring within the fovea. This chapter outlines the results of these experiments.

## METHODS

A reliable behavioral technique was developed for the accurate placement of single, small spot exposures onto predetermined retinal areas in an awake, task-oriented animal. This method did not require the use of anesthesia or undue physical restraint.<sup>27</sup> Instead, the animal was trained to maintain fixation on a small target that was placed in the middle of a rear projection screen.<sup>26,27</sup> The animal received a positive cue as long as it maintained its fixation on the targets and was negatively reinforced for failure to do so. The impact of random, involuntary, and voluntary eye movements was further reduced by using relatively short-duration exposures that were presented while the animal was actively engaged in a threshold visual discrimination task that required central fixation on a single known critical feature of briefly presented visual targets.

### Subjects and Apparatus

Adult male rhesus monkeys with normal vision were used as participants. The animals were tested in a portable restraint device that was also used to transport the animal to and from the housing colony.<sup>28</sup> A custom-fitted helmet molded from high-impact plastic and equipped with an inner, high-density foam liner with an inflatable air bladder stabilized the monkey's head without undue force or discomfort. An opaque facemask with adjustable iris diaphragms was aligned with the animal's line of sight. This required the monkey to voluntarily align its pupil with an artificial pupil to view the test screen. With positive reinforcement, the animals were quickly trained to voluntarily leave their home cages and enter the restraint apparatus.

### Discrimination Task

Animals were trained to press a lever whenever they detected the presence of a Landolt ring ("C"). These incomplete rings were randomly positioned within a series of equally sized gapless rings ("O"). Individual rings were successively projected onto a rear projection screen placed 1 m in front of an artificial pupil that

was mounted onto the animal's head restraint. The animal's failure to press the lever to the Landolt ring when presented (*miss*), or if the lever was pressed during presentation of a gapless ring (*false alarm*), resulted in presentation of a brief discriminative tone and, on a variable reinforcement schedule, the administration of a brief electrical shock.

Threshold acuity was derived using a tracking technique. In this technique, if the subject correctly detected the Landolt ring (*hit*) by pressing a lever, the next series of Landolt rings and gapless rings were 10% smaller, whereas an incorrect detection (*miss*) produced presentation of rings 10% larger. The critical feature of each Landolt ring that distinguished it from corresponding gapless rings varied from a 0.25- to

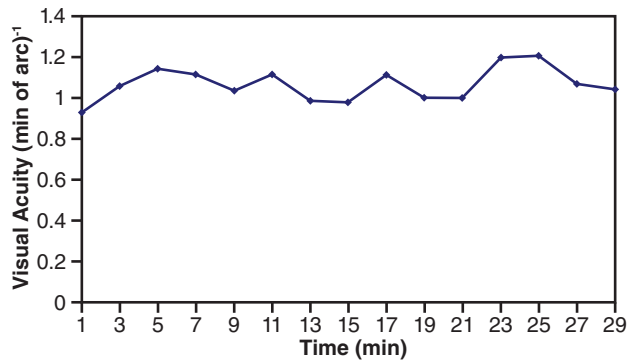


**Figure 4-1.** Preexposure baseline acuity. The animal's threshold acuity was averaged in consecutive 2-min intervals using maximum photopic viewing conditions. Established acuity level of  $1.1 \text{ (min of arc)}^{-1}$  or a Snellen acuity of 20/18 was typical for our animals under these viewing conditions. Ongoing acuity was tracked for 30 min without a break; during this period, average threshold acuity for any running 2 min never dropped below  $1.0 \text{ (min of arc)}^{-1}$  once maximum threshold level was established. Similar to other animals, this subject's false-positive response rate was <10%. No negative reinforcement was applied during the test period. A criterion of two successive misses to threshold Landolt rings was typically used before shock was applied to the third consecutive miss. Normally, a well-trained animal avoided negative reinforcement altogether once motivated to perform.

30-min visual angle in 10% steps. The position of the gap was always in the same location on the viewing screen. By varying the payoff matrix used during training, the number of false alarms was remarkably low (<10%), and animals maintained stable acuity for periods in excess of 45 min of testing. In well-trained animals, baseline visual acuity varied from a Snellen acuity of 20/25 to 20/12, depending on the parameters of the viewing conditions (Figure 4-1). Darkened rings of various diameters were projected onto different wavelength and intensity backgrounds to determine any selective spectral, contrast, or brightness acuity effects.<sup>5</sup>

### Laser Exposures

Several different laser systems were used at various times during the course of this research. Initially, He-Ne (helium-neon), krypton, and argon CW lasers were used to generate relatively long-duration exposures (50–500 ms) of different wavelengths; later, in our research, a Nd:YAG (neodymium-doped yttrium aluminum garnet) pulsed laser was used to

produce Q-switched pulses for shorter-duration, higher-energy exposures. Each of these laser systems also varied in output wavelength. The lasers were positioned on an optical bench outside the test chamber. The beam was first directed through several neutral density filters and a manual safety shutter before passing through an electronic shutter and beam splitter. A portion of the attenuated beam was incident upon an absorbing disc calorimeter for monitoring exposure energy. The transmitted portion of the beam was diverted by a front surface mirror and passed through a variable beam expander and a convex lens placed in front of the animal's pupil. A coated pellicle beam splitter placed 5 cm in front of the lens was positioned at the intersection of the diverging laser beam and the light beam from the viewing screen. The laser beam was positioned such that it was presented to the animal coaxial with a line between the artificial pupil and the gap in a specified, threshold Landolt ring; or, in the case of off-axis exposures, it was positioned 1° above the gap in the specified Landolt ring. Beam diameter could be varied from <50 to >800  $\mu\text{m}$  on the retina.

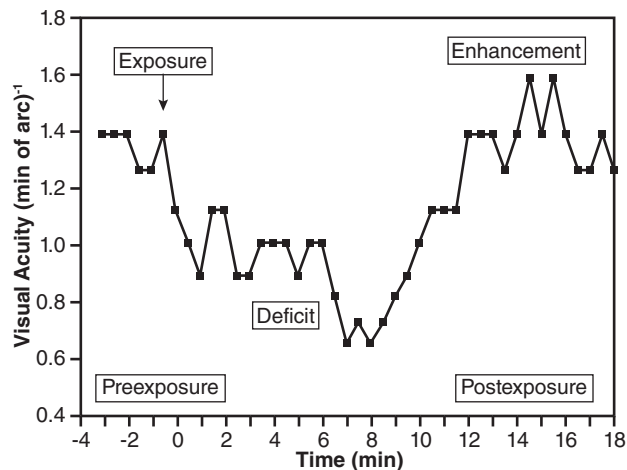


**Figure 4-2.** Sample raw data demonstrating immediate drop in visual acuity following laser exposure. The *ordinate* indicates sizes of the gaps in presented Landolt rings measured in reciprocal minutes of arc. The *abscissa* represents time (in minutes) of presentation of threshold Landolt rings relative to exposure (marked as 0) based on our tracking technique. Two, 0.1- $\mu\text{J}$  Q-switched pulses, 300  $\mu\text{m}$  diameter, were presented on-axis to produce the transient acuity deficit shown here. Only 4 min of preexposure acuity is shown. Normally, preexposure was measured until the animal established a stable baseline (typically within approximately 10 min) before laser exposure; baseline testing continued for another 30 min or until the animal established a stable postexposure acuity, whichever came first.

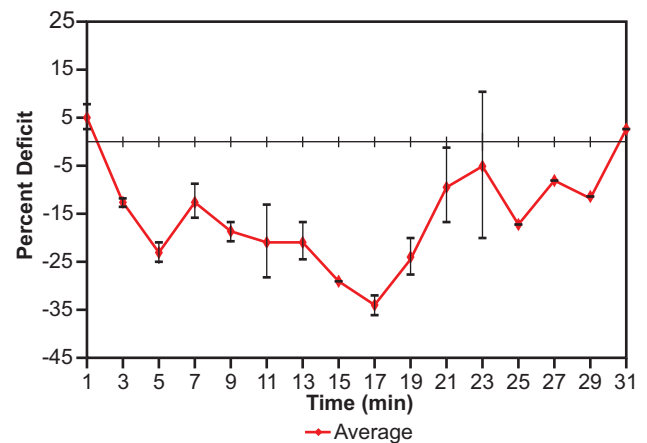


**Figure 4-3.** Average recovery functions in visual acuity following low-level (0.1- $\mu\text{J}$ ), multiple-pulse exposures (small spot size). This animal was exposed to two Q-switched pulses presented on-axis within a 100-ms window. Retinal spot size was 150  $\mu\text{m}$ ; postexposure acuity was measured immediately after exposure (marked as 1 min on the abscissa) and computed continuously in 2-min intervals for the next 31 min. Only two 532-nm pulses (exposure) were presented per session (day); the recovery function shown represents the average postexposure deficit of four separate exposure sessions over as many days. The animal's postexposure acuity was plotted relative to its preexposure baseline as percent deficit. The *vertical bars* through each data point (diamonds) represent the range of acuity variability (minimal and maximal) observed for the four separate exposure sessions.

The number of pulses presented was controlled by a remote electronic shutter placed in the beam pathway. Varying the duration of the shutter from <50 to >250 ms resulted in the presentation of one to six pulses within the brief exposure session. Longer-duration exposures were avoided to eliminate the impact that voluntary eye movements could have on the position of the exposure on the retina.

All exposures were presented while the animal was tracking its threshold visual acuity and immediately after the animal had correctly detected the minimal gap in the Landolt ring. Observations of animals working under these conditions have shown that they typically maintain their fixation on the screen for several seconds after lever pressing. Normally, animals were exposed only once per day and only after their preexposure baselines were reliably established. The animal's postexposure acuity was followed until it regained its preexposure level or the elicited deficit had stabilized (Figure 4-2). All acuity measurements were made under monocular viewing conditions using both high-luminance (*photopic*) and low-luminance (*scotopic*) chromatic and achromatic targets. Figure 4-3 demonstrates the reliability of derived recovery functions using this technique. In this example, the same animal was exposed on separate sessions to low-level,

repetitive Q-switched pulses that each sustained 150  $\mu\text{m}$  on the central fovea. The total exposure duration for each session was 100 ms. The average time for full recovery was approximately 30 min, and the average initial deficit ranged from 20% to 25% within the first 5 min after exposure.

### Data Analysis

Each animal's preexposure average acuity was derived over a 15- to 20-min period at the beginning of each exposure session. To determine any motivational or lingering exposure effects, the average preexposure acuity, as well as degree of variability (number of different-sized gaps represented), was compared to previous session baselines and to those from the animal's control eye. Postexposure acuity was analyzed in 2-min-long intervals beginning immediately after the exposure. For each interval, the percent deficit was derived by comparing the average acuity during this 2-min period to the overall preexposure acuity derived for the animal immediately prior to exposure. In those cases where prolonged acuity changes were noted, no additional exposures were made, and postexposure acuity was measured using different spectral and contrast conditions.

## RESULTS

When either large (200–500  $\mu\text{m}$ ) diameter foveal exposures were presented for a brief period (single Q-switched pulse) or when small (50–150  $\mu\text{m}$ ) diameter foveal exposures were presented for relatively prolonged exposure periods using multiple Q-switched pulses (up to 250 ms), the immediate impact on visual acuity was relatively dramatic. These types of Nd:YAG exposures produced deficits reminiscent of those produced by short-duration (50–100 ms) CW argon and HeNe flashes as previously reported elsewhere.<sup>29</sup> In these millisecond time-domain exposures, where full recovery was possible, immediately after exposure the animal's acuity typically decreased significantly (20%–80% of preexposure acuity) and remained depressed for some time (4–20 min) before gradually recovering to its preexposure baseline. Both the size of the initial deficit and the total time for recovery were dependent on the parameters of the exposure that included its energy density, spot diameter, duration, and position on the retina. For some exposure conditions defined as being within the transition zone between temporary and permanent effects, the initial deficits were as high as 80%, and full recovery took as long as several days. Typically below the transitional zone, the magnitude of the initial deficit was largely dependent on the size

and location of the exposure site, whereas the duration of the deficit was dependent on exposure energy. For energy densities near or within the transitional zone, the overall impact (size of initial deficit and time for recovery) of individual exposures gradually increased with repeated exposures even though these exposures were separated from each other by as much as several days. Often, these cumulative effects produced permanent shifts in postexposure acuity that were only noted after the fourth or fifth exposure at a specific energy density.

When single Q-switched pulses of small diameters (< 50  $\mu\text{m}$ ) were presented, however, there was little obvious decrement in visual acuity at or below the  $ED_{50}$  level. Under these nanosecond time-domain exposures, the animal was able to maintain a stable acuity after the exposure and throughout the postexposure session. With larger-diameter (>150- $\mu\text{m}$ ) exposures, the adverse impact of single pulses on visual acuity was more evident and generally the same as the transient deficits produced by smaller-diameter exposures presented either with CW irradiation (100-ms flashes) or with multiple Q-switched pulses in rapid succession of each other. With either type of condition, immediately after exposure, the animal's baseline acuity dropped

and remained depressed for some time before postexposure acuity gradually began to return to its preexposure baseline. Both the magnitude and duration of the observed visual deficits were related to the amount of retinal area involved (exposure spot size) and to the number of Q-switched pulses presented. Increasing the

power density of single Q-switched pulses for small-diameter exposures produced little additional impact on the animal's derived acuity, even for energy levels significantly above ( $10\times$ – $100\times$ ) the  $ED_{50}$ .

With larger-diameter exposure sites, however, the energy of the pulses clearly influenced the duration

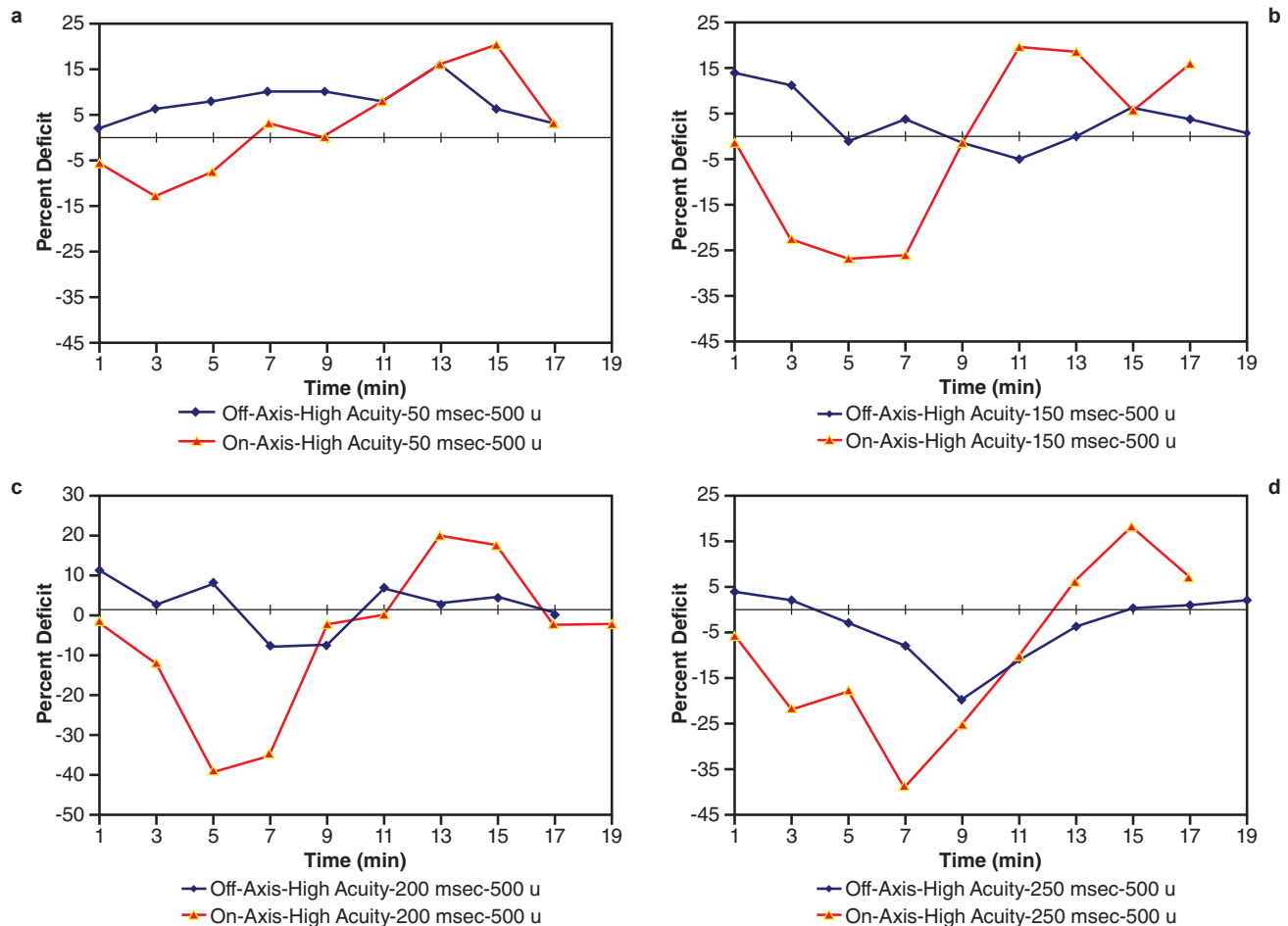


**Figure 4-4.** (a) On- and off-axis exposures to single Q-switched pulses at energy levels below the transition zone for permanent deficits (large spot size). One 532-nm Q-switched pulse was presented per session (day) within a 50-ms exposure window either coaxial with (on-axis) or temporal (off-axis) to the gap in a threshold Landolt ring. The energy of the pulse was  $0.1\ \mu\text{J}$ , and the beam diameter on the retina was approximately  $500\ \mu\text{m}$ . Acuity is plotted as percentage of preexposure acuity for each running 2 min following exposure. *Triangles* represent acuity following an on-axis exposure; *diamonds* represent acuity following an off-axis exposure. (b) On- and off-axis exposures to multiple (3) Q-switched pulses at energy levels below the transition zone for permanent deficits (large spot size). Three 532-nm Q-switched pulses were presented within a 150-ms exposure window either coaxial with (on-axis) or temporal (off-axis) to the gap in a threshold Landolt ring. The energy of the pulse was  $0.1\ \mu\text{J}$ , and the beam diameter on the retina was approximately  $500\ \mu\text{m}$ . Acuity is plotted as a percentage of preexposure acuity for each running 2 min following exposure using our tracking technique. *Triangles* represent the acuity following an on-axis exposure; *diamonds* represent acuity following an off-axis exposure. (c) On- and off-axis exposures to low-level, multiple (4, 5) Q-switched pulses at energy levels below the transition zone for permanent deficits (large spot size). Repetitive, 532-nm Q-switched pulses were presented within a 200-ms (c) or 250-ms (d) exposure window either coaxial with (on-axis) or temporal to (off-axis) the gap in a threshold Landolt ring. The energy of each exposure was  $0.1\ \mu\text{J}$ , and the beam diameter on the retina was approximately  $500\ \mu\text{m}$ . Acuity is plotted as a percentage of preexposure acuity for each running 2 min following exposure using our tracking technique. *Triangles* represent the acuity following an on-axis exposure; *diamonds* represent acuity following an off-axis exposure.

of the deficit, as well as the likelihood of full recovery within the remaining time of the test session. The impact of multiple exposures under this condition often became prolonged and sometimes permanent for Q-switched pulses above the  $ED_{50}$ . But, unlike the millisecond time-domain exposures, no transitional zone was found where cumulative effects could be noted for repeated exposures when single pulses of very small spot sizes ( $<150\ \mu\text{m}$ ) were used. Control trials in which low-energy exposures were positioned as little as  $1^\circ$  off of the animal's point of central fixation dramatically reduced the overall adverse impact of laser irradiation. Measuring immediate postexposure acuity under different viewing conditions (high- vs low-contrast or achromatic vs chromatic) produced little relative difference in either the percent deficit or the duration of transient deficits, and contributed little to a fuller understanding of the nature of these changes. In those exposures where permanent changes were noted, however, postexposure acuity was often significantly different for different contrast, luminance, and chromatic targets; these types of long-term changes did provide some discernment of the location and nature of the damage produced.

The transient impact of retinal exposure position on visual acuity is shown in Figure 4-4. Even with relatively large-diameter ( $500\ \mu\text{m}$ ), low-energy, Q-switched exposures, the magnitude and duration of transient deficits were small for single-pulse exposures compared to those deficits produced by multiple pulses or CW exposures. In Figure 4-4, the beam was positioned either coaxial with the gap in a threshold Landolt ring (*on-axis*) or  $1^\circ$  temporal to the gap (*off-axis*). Off-axis exposures should have little impact on foveal function because they should expose areas outside of the central fovea. In Figure 4-4a, a single, low-level, Q-switched pulse was presented either on-axis or  $1^\circ$  off of the animal's fixation point. For the on-axis exposure, the animal's visual acuity decreased by approximately 15% during the first 3 min following irradiation before quickly returning to its preexposure baseline within 7 min of exposure. This visual deficit was rather minor and transient compared to those elicited by millisecond time-domain flashes or multiple Q-switched pulses.

Consistent with other examples of low-level exposures (see Figure 4-4, b-d), immediately after the animal's postexposure acuity deficit recovered, the animal's acuity became temporarily enhanced for several minutes before gradually returning to its normal preexposure baseline. In this example, the animal's transient enhancement was approximately 20% better than its baseline, an increase in visual acuity to  $1.44\ (\text{min of arc})^{-1}$  or a Snellen acuity of 20/14. This

enhancement effect gradually began within 11 min of the exposure and lasted approximately 8 min before the animal's acuity again stabilized at its preexposure level, some 17 min after exposure. The off-axis exposure produced no immediate deficit or delayed enhancement in visual acuity. This animal was able to maintain its preexposure acuity level after exposure and, if anything, slightly improved during the course of the 20-min test session. For the most part, postexposure acuity was elevated by approximately 5% during the first 13 min after exposure. Although minor, this shift occurred consistently and was outside this animal's normal within-session variability. In Figure 4-4b, the same comparison of on- and off-axis exposures was made except in this example the number of Q-switched pulses presented was increased from one pulse to three pulses within a 150 ms exposure window. Again, for the off-axis exposure, little if any deficit was noted during the 20-min postexposure session; but, for the on-axis exposure, an immediate and significant drop in visual acuity was noted. For the on-axis condition, the initial postexposure deficit was  $>25\%$ , and the animal's acuity remained depressed for approximately 7 min before returning to its preexposure acuity in 9 min. Similar to the previous example (see Figure 4-4a), the elicited visual deficit was followed by a brief, but significant, enhancement in acuity that lasted several minutes before the animal's acuity stabilized at its preexposure level. Overall acuity effects were the same for single and repetitive Q-switched pulse conditions.

The presentation of more on-axis pulses within a restricted time frame produced even larger initial deficits without significantly affecting the overall duration of the recovery function. With four Q-switched pulses (see Figure 4-4c), for example, the initial deficit increased to  $>40\%$  (with a Snellen acuity of 20/28), and the animal's acuity remained depressed for approximately 10 min before gradually returning to its preexposure acuity level. Similar to the previous examples, the elicited visual deficit was again followed by a brief, but significant, enhancement in acuity before it stabilized at its preexposure level. With five pulses (see Figure 4-4d), the initial deficit was closer to 45% of its preexposure level and reached its maximum within the first 7 min following exposure before gradually returning to its baseline within 13 min. The animal again demonstrated hyperacuity for the last 4 min of postexposure testing. The off-axis exposures for one to five pulses were virtually identical to each other and showed no consistent or significant drop in acuity either during or immediately following laser exposures.

The impact of retinal exposure position on postexposure acuity appears independent of the exposure time domain. Using millisecond time-domain expo-

ures, we have demonstrated a similar decrease in effect because the exposure site is positioned farther away from an animal's point of central fixation. For example, in Figure 4-5, a series of recovery functions from four different 100-ms exposures is shown where the exposure position relative to the animal's fixation point varied from on-axis to as much as 6° off-axis. Somewhat independent of their actual position on the retina, these longer duration CW exposures also involved a larger retinal region than the previous Q-switched pulses. Continuous and random eye movements during the exposure, even when the animal was fixating on the visual target, resulted in a larger area of involvement when millisecond as opposed to nanosecond time-domain exposures were made. When multiple Q-switched pulses were presented over the same 100 ms period, only two 15 ns pulses would normally be delivered. Hence, only two discrete areas were exposed in the nanosecond time domain. In Figure 4-5, an animal was exposed to a series of different exposures positioned varying distances away from the point of central fixation. Again, only one exposure was presented per session. The sham

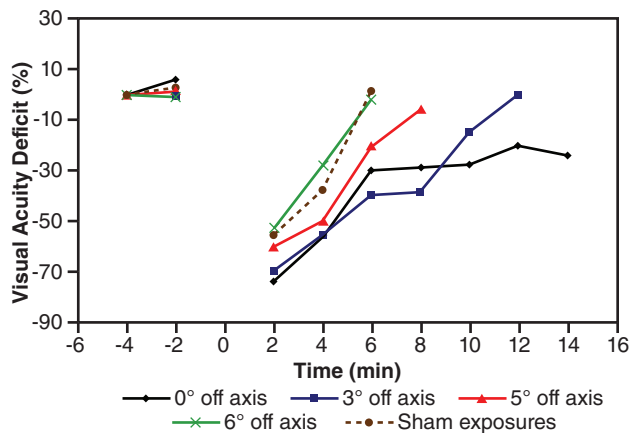


**Figure 4-5.** Recovery functions following different continuous wave exposures at various eccentricities. This animal was exposed to single, 100-ms, 150- $\mu\text{m}$ , 647-nm flashes from a krypton continuous wave laser. The spot was positioned on-axis (0° [diamonds]) and off-axis (3° [squares], 5° [triangles], and 6° [crosses]) to the gap in a threshold Landolt ring. Immediately after exposure, the size of the target (discriminanda) was manually adjusted to the size normally able to be just detected after an on-axis exposure. Postexposure acuity was then tracked for each running 2 min until the animal achieved its preexposure baseline acuity. Acuity was measured using high-contrast targets on an achromatic background. The energy of the exposure was below the transitional zone between temporary and permanent effects. The sham exposures (circles) represent the time it took using our tracking technique for the animal to reestablish its baseline acuity when no laser irradiation was presented.

exposure represents the control where no exposure was made, but where the discriminanda size was shifted to the approximate level that an on-axis exposure could first be visible. This curve thus represents the time it takes for a subject using our tracking technique to return to baseline without making any discrimination errors. The recovery functions for exposures of 5° and 6° off-axis were virtually identical to that observed in the sham condition. With a 3° off-axis exposure, recovery was delayed by approximately 6 min; for an on-axis exposure, recovery in visual acuity was not complete within the 14-min postexposure session. Follow-up postexposure testing in this animal revealed no lasting deficit or lingering effects from these or other exposures at this power density.

Using millisecond time-domain exposures, we have demonstrated the effects that variations in exposure duration can have on the duration of the recovery function when minimal diameter spots (<50  $\mu\text{m}$ ) are

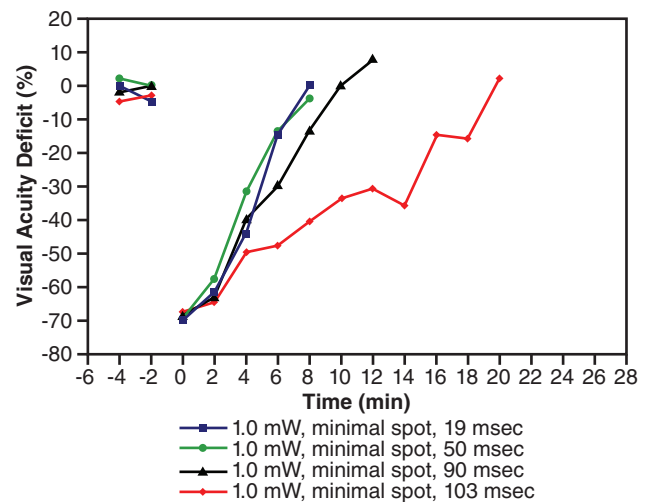


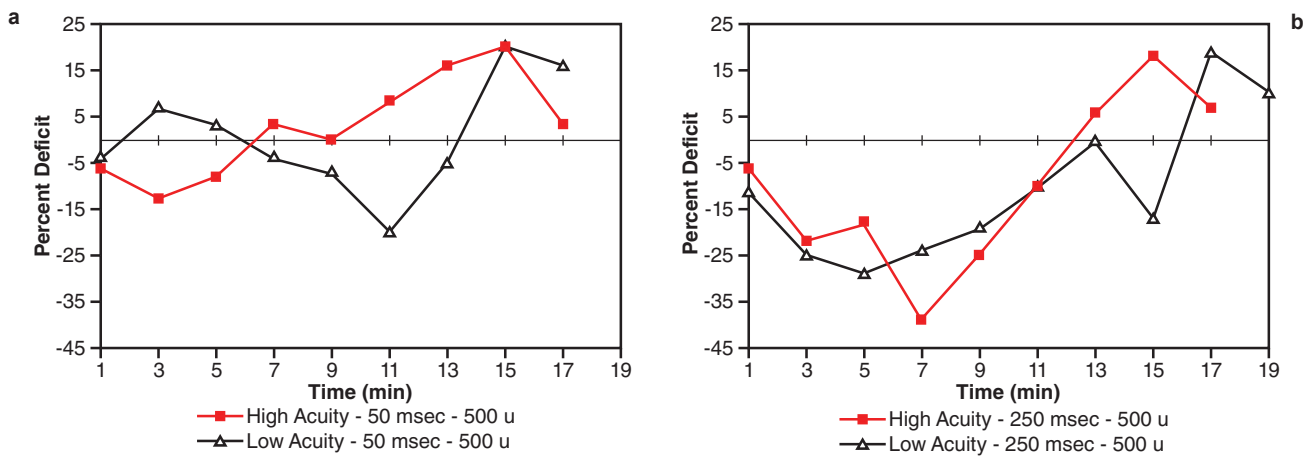
**Figure 4-6.** Effects of different continuous wave laser exposure durations (millisecond time domain) on postexposure visual acuity. The individual recovery functions were derived for one animal exposed repeatedly over different days to 1.0-mW flashes from an argon (514.5 nm) laser. Each exposure was presented coaxial with a gap in a threshold Landolt ring and produced an approximate 50- $\mu\text{m}$  spot on the retina. Each data point represents the average running 2-min postexposure intervals of several separate exposure sessions. The duration of the exposures was produced by a programmable electronic shutter whose pulse duration was measured on a standard oscilloscope. Durations of 19 ms (squares), 50 ms (circles), 90 ms (triangles), and 103 ms (diamonds) are shown. Similar to Figure 4-5, the size of Landolt rings was manually increased immediately following exposure to the level expected for this type of exposure. Using our tracking technique, the animal then adjusted its threshold acuity until it returned to its preexposure baseline.

used. In Figure 4-6, the individual recovery functions are shown for four different duration exposures ranging from 19 to 103 ms. As the figure shows, recovery to flashes of 19 and 50 ms are almost immediate (within 4–8 min) and represent the recovery times not significantly different from the sham condition shown in Figure 4-5. For longer or repeated exposures using either CW lasers or multiple pulses from a Q-switched energy source, however, the duration of the recovery function for minimal diameter spots was similar to those observed when larger diameter exposures were administered. From these data, it would appear that the consequence of one longer, 103 ms flash was slightly greater than that of two 50 ms flashes presented 2 min apart. Such might be the case if eye movements alone were the prevailing catalyst for this type of effect.

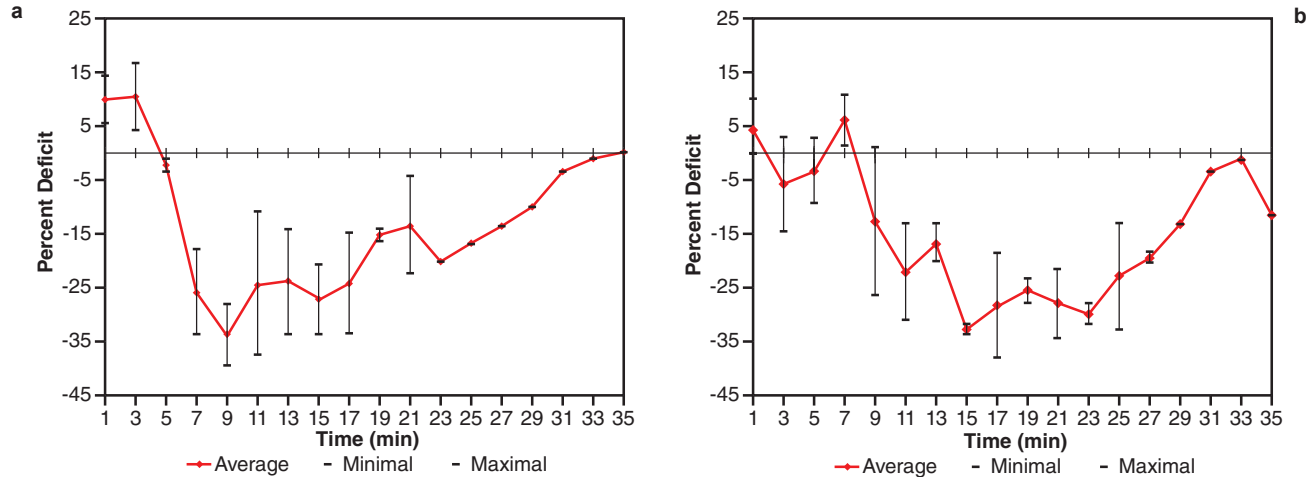
The influence of the acuity task on delineating the magnitude and duration of the transient visual deficit is shown in Figure 4-7 for low-level laser irradiation. In Figure 4-7, the animal's pre- and postexposure acuities were measured using either a high-luminance background (high acuity) or a low-luminance background (low acuity) against darkened visual targets. Typically, an animal's preexposure acuity in the high-acuity (high-luminance) condition was approximately 1.2 (min of arc)<sup>-1</sup> or had a Snellen acuity of 20/17, whereas preexposure acuity derived under the low-acuity (low-luminance) condition was approximately 0.65 (min of arc)<sup>-1</sup> or had a Snellen acuity of 20/31. Our animals' preexposure acuity varied little from session to session

and was extremely consistent within a testing session when no exposure was made.

Generally, the recovery functions for repeated exposures using the same conditions (either exposure or performance) were remarkably similar, especially when large-diameter spots and multiple Q-switched pulses were presented. When single Q-switched exposures were used and/or when the diameter of the exposure on the retina was minimal (< 50 μm), the elicited deficit was smaller, and more variability existed across exposure sessions and between animals. The observed increased within-subject variability likely represents the degree to which the exposure was centered on the fovea and the extent to which surrounding foveal regions were still functional. The between-animal variability also likely represents the degree to which different animals use various strategies to detect threshold targets after exposure, especially when off-axis fixations are required. As expected, deriving postexposure acuity functions using percent change from preexposure acuity (vs absolute acuity) considerably reduced the between-subject variability. In spite of generally higher energy densities for Q-switched pulses, more variable recovery functions were noted in this study using nanosecond time-domain exposures than in previous studies with lower-energy CW laser exposures in the millisecond time domain. The majority of exposures in this study, however, involved smaller-diameter spots and briefer duration exposures that could easily explain the observed increased variability.



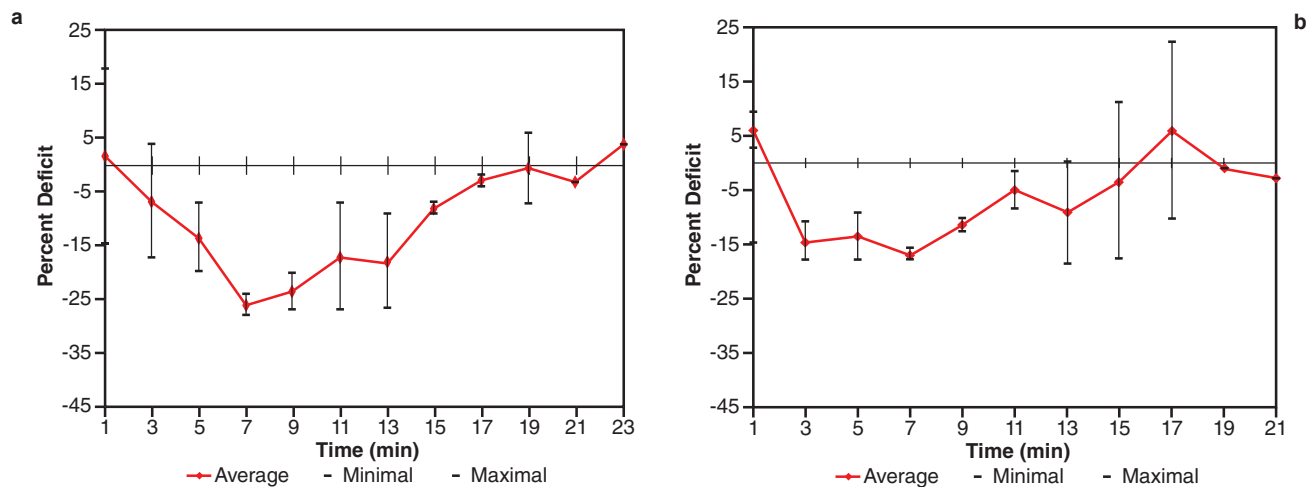
**Figure 4-7.** (a) Effects of measuring postexposure acuity using high- and low-luminance targets following Q-switched Nd:YAG (neodymium-doped yttrium aluminum garnet) laser exposures. In each figure, the animal was exposed to a single Q-switched pulse (a) or to five Q-switched pulses within a 250-ms window (b). The energy per pulse was 0.1 μJ presented coaxial with the gap in a specified Landolt ring (on-axis). Each pulse produced an exposure diameter of approximately 500 μm on the retina. Postexposure acuity was measured in 2-min intervals for 20 min after each exposure, using different-sized Landolt rings projected onto white light backgrounds of two different luminance levels. The differences in luminance density between the high and low backgrounds was 3.0 log units. *Squares* represent postexposure acuity for high-luminance targets; *triangles* represent postexposure acuity for low-luminance targets.



**Figure 4-8.** (a) Average recovery functions derived for different luminance backgrounds after low-level, multiple (5) Q-switched Nd:YAG (neodymium-doped yttrium aluminum garnet) laser exposures (small spot size = 150  $\mu\text{m}$ ). A comparison of the recovery functions of one animal is shown for both high- (a) and low-luminance (b) backgrounds for the darkened Landolt rings. This animal was exposed to five Q-switched pulses from a Nd:YAG laser presented within a 250-ms window. Only one series of 532-nm pulses (exposure) was presented per session (day); each recovery function represents the average of four separate exposure sessions. The *vertical bars* through each data point (diamond) represent the range (minimal and maximal) of acuity variability observed for the separate exposure sessions presented. Retinal spot size was 150  $\mu\text{m}$  and energy per pulse was 0.1  $\mu\text{J}$ .

In Figure 4-8, an average recovery function derived for one animal from four separate exposure sessions is shown for both high- and low-acuity criterion. No statistically significant difference was found between the

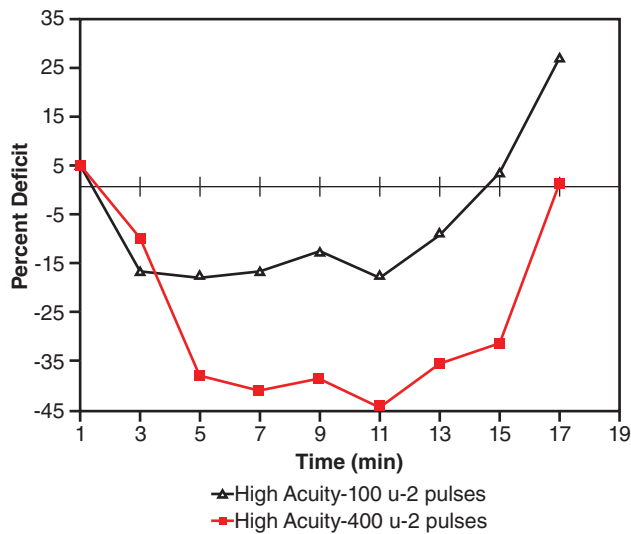
two recovery functions. For each criterion, the animal's visual acuity decreased rather significantly within 7 to 10 min after exposure and remained depressed for the next 20 min before gradually returning to its preexpo-



**Figure 4-9.** (a) Average recovery functions derived for different luminance backgrounds after low-level, multiple (4) pulse exposures (large spot size = 200  $\mu\text{m}$ ). A comparison of the recovery functions of one animal is shown for both high- (a) and low-luminance (b) backgrounds for the darkened Landolt rings. This animal was exposed to four Q-switched pulses from a Nd:YAG (neodymium-doped yttrium aluminum garnet) laser presented within a 200-ms window. Each recovery function represents the average of four separate exposure sessions; *vertical bars* through each data point represent the range of variability (minimal and maximal) observed for the separate exposure sessions presented. Retinal spot size was 200  $\mu\text{m}$ , and energy per pulse was 0.1  $\mu\text{J}$ .

sure level within 35 min of exposure. In the recovery functions shown in Figure 4-8, the initial visual deficit appeared to occur earlier during the postexposure period when high-acuity criteria, as opposed to low-acuity criteria, were used. However, in Figure 4-9, no significant differences were found between the time course of the initial deficit and acuity criterion used.

In Figure 4-9, the diameter of the exposure on the retina was increased from 150 to 200  $\mu\text{m}$ , whereas the number of pulses was decreased from five Q-switched pulses presented within a 250-ms exposure window to four pulses presented within a 200 ms window. In spite of these changes in exposure parameters, both the magnitude of the initial deficit and time for full recovery for each derived recovery function did not change significantly from those recovery functions as previously shown. For the high-acuity criterion (see Figure 4-9a), postexposure acuity dropped to 25% of its preexposure level approximately 7 min after exposure. During the next 14 min, the animal's acuity gradually improved, and eventually returned and stabilized at its preexposure baseline. For the low-acuity criteria (see



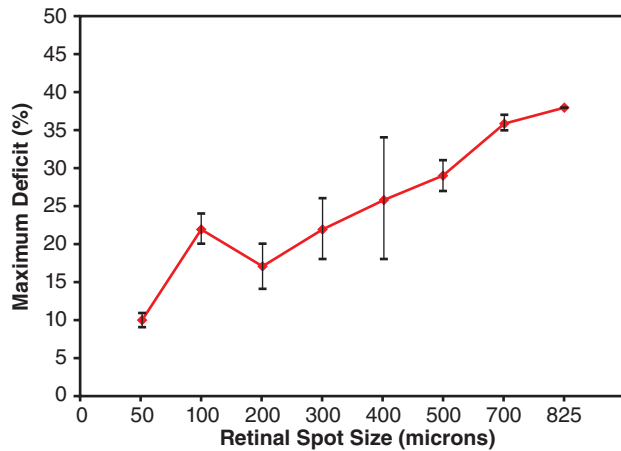
**Figure 4-10.** Comparison of two different spot sizes (100 vs 400  $\mu\text{m}$ ) on the initial magnitude and total duration of the visual deficit. Two low-energy, Q-switched pulses from a Nd:YAG (neodymium-doped yttrium aluminum garnet) laser were presented coaxial with the gap in a threshold Landolt ring under maximum photopic conditions. Each pulse produced either a 100- or 400- $\mu\text{m}$  diameter spot on the retina. Only one exposure (two consecutive pulses) was presented per day; acuity was measured as a percentage of preexposure acuity for successive 2-min postexposure intervals. *Triangles* represent high acuity: 100  $\mu\text{m}$ , 2 pulses; *squares* represent high acuity: 400  $\mu\text{m}$ , 2 pulses.

Figure 4-9b), neither the initial deficit nor the size of the maximum deficit was as large as that shown for the high-acuity criterion; but, here again, the immediate deficit in visual acuity stabilized in approximately 7 min before finally returning to its preexposure baseline within 17 min of exposure. The variability in results across different exposure sessions was actually quite small, as represented by the error bars in Figure 4-9a and Figure 4-9b. Each of these curves represents the average of four separate exposure sessions. Similar results were also observed with other spot sizes and number of Q-switched pulses at this energy level.

Differences in the diameter of the retinal laser exposure did have an impact on the likelihood of observing a deficit and on the magnitude of any observable acuity shift. As previously reported, for very small-diameter Q-switched pulses, deficits observed were often very small and transient in spite of the fact that they were presented on-axis and were relatively high in energy. This minimal consequence was most evident when only 1 or 2 ns pulses were presented. When larger spot sizes were used, larger and more sustainable visual deficits were elicited. The comparison of deficits produced by two different spot sizes is shown in Figure 4-10.

In this figure, the animal was exposed on two separate occasions to two Q-switched pulses of low-energy light that generated either a 100- or 400- $\mu\text{m}$  diameter spot on the retina. These exposures were presented coaxial with the gaps in threshold Landolt rings, and postexposure visual acuity was measured using high-luminance targets. There was a significant decrease in the animal's visual acuity immediately after either diameter spot. For the 100  $\mu\text{m}$  diameter spot, the initial visual deficit leveled off after 4 min and remained at this depressed level for approximately 12 min before gradually returning to its preexposure level in 16 min. The average deficit that was sustained during the initial phase of the recovery was 15%. For the 400  $\mu\text{m}$  diameter spot, the animal's visual acuity also immediately dropped and within 6 min had reached a maximum deficit of 45%. The animal's deficit remained at this acuity level for approximately 12 min before the visual deficit gradually returned to its preexposure baseline in 18 min. The time course of the recovery curves for these two different exposures was remarkably similar, differing only in the degree of the initial deficit.

A direct comparison of the size of the initial acuity deficit, with eight different retinal spot sizes, is shown in Figure 4-11. For a relatively small (50  $\mu\text{m}$ ) diameter spot, little or no deficit was observable using our behavioral paradigm; but, as the spot diameter increased, an almost monotonic relationship developed between the magnitude of the maximum deficit and retinal spot size. In this example, the animal was exposed to only a single,



**Figure 4-11.** Effects of retinal spot size on the magnitude of the initial maximum postexposure acuity deficit. This subject was exposed daily to a single 3- $\mu$ J, Q-switched pulse from a Nd:YAG (neodymium-doped yttrium aluminum garnet) laser. All exposures were presented on-axis. Acuity was measured using high-contrast, achromatic targets. Each data point represents the mean of five different exposures over as many days; *vertical bars* represent range of deficits observed for each of the eight different spot sizes. The *abscissa* represents different retinal spot sizes varying from 50 to 825  $\mu$ m; the *ordinate* represents maximum deficit relative to the animal's preexposure acuity produced by the laser exposure.

15 ns pulse for each exposure diameter. This virtually eliminated any impact that voluntary or involuntary eye movements might have on the actual size of the retinal irradiation. When the exposure duration was longer (millisecond domain) or multiple pulses (nanosecond domain) were presented sequentially, we have always assumed that ongoing eye movements actually created larger retinal exposure areas. In Figure 4-11, the calculated diameter of the exposure site on the fovea varied from approximately 50 to 825  $\mu$ m. The largest-diameter spots likely irradiated the animal's entire fovea and produced a significant loss in photopic acuity that peaked at about 45% of the animal's preexposure acuity level. For smaller areas of retinal involvement, the deficit was proportionally smaller. Overall, little variability was observed between exposures of the same diameters. A random design of different spot sizes was presented over different test sessions. A somewhat heightened deficit was observed for spot diameters of 100  $\mu$ m in comparison to spot diameters of 50 and 200  $\mu$ m.

Doubling the number of Q-switched pulses presented within a 100 ms exposure window produced a less dramatic overall impact than retinal spot size had on determining the magnitude of the initial deficit. In Figure 4-12, a similar comparison of retinal spot size is shown for a double rather than a single Q-switched

pulse, although in this example the different graphs represented different exposure energies. The maximum deficit occurred after only tripling the retinal spot size in most cases, especially for those energy densities above 0.5  $\mu$ J. The magnitude of the maximum deficit varied from <10% to >50% of its preexposure level. In this example, the energy per pulse varied from 0.1  $\mu$ J to 5.0  $\mu$ J for the six different spot diameters used. Under these exposure conditions, the energy per pulse appeared to have little consistent impact on the magnitude of the initial deficit. For example, when 50  $\mu$ m spot sizes were used, the initial deficit was quite small (<10%) and differed little regardless of the energy of the pulses. Increasing spot diameters to 100  $\mu$ m or more changed the magnitude of the maximum deficit from 10% to >50% of its preexposure level. However, little systematic change in the magnitude of the initial deficit was observed for spot sizes that varied as much as 600  $\mu$ m from each other. Typically, the maximum deficit was observed within the first 5 to 8 min after exposure, and full recovery was complete within 30 to 40 min of exposure. No long-term shift in acuity was observed for any of the exposures used to produce the data in Figure 4-12.

As might be expected, the area of involvement was related not only to the magnitude of the initial deficit, but also to the total time for recovery. Figure 4-13 dem-

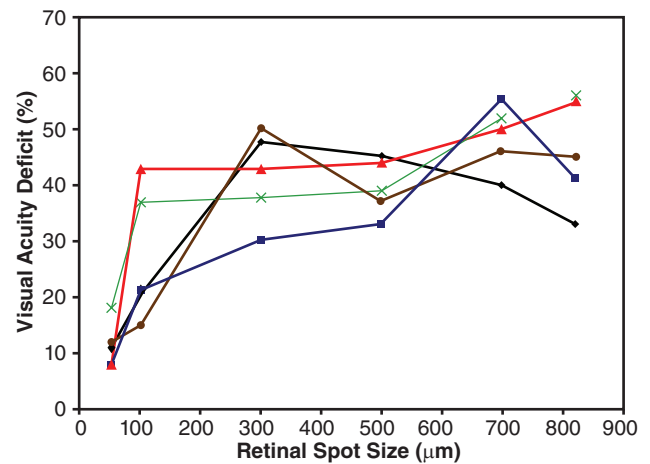


**Figure 4-12.** Effects of different (5) energy pulses and spot diameters (6) on the magnitude of maximum postexposure acuity deficit. This subject was exposed daily to two Q-switched pulses within a 100-ms window from a Nd:YAG (neodymium-doped yttrium aluminum garnet) laser. All exposures were presented on-axis; acuity was measured using high-contrast, achromatic targets. For each of the six diameter exposures, the pair of 532-nm pulses varied in energy density from 0.1 to 5.0  $\mu$ J (*diamonds*: 0.1  $\mu$ J, *squares*: 0.5  $\mu$ J, *triangles*: 1.0  $\mu$ J, *crosses*: 3.0, and *circles*: 5.0  $\mu$ J).

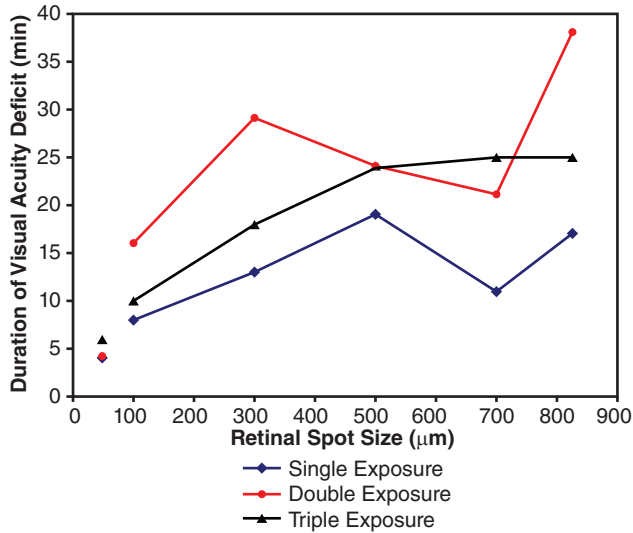


**Figure 4-13.** Duration of visual deficit for single, double, and triple Q-switched Nd:YAG (neodymium-doped yttrium aluminum garnet) pulses. This animal received only one exposure per day; that exposure varied in either the number of Q-switched pulses presented (1–3) or in the size of the spot on the retinal surface. The diameter of the on-axis exposure shown on the *abscissa* varied from <50 to 825 µm, and the duration (minutes) of the postexposure deficit as a percentage of preexposure acuity is plotted on the *ordinate*. The energy of these pulses was several log units below the ED<sub>50</sub> (effective dose for 50% of the population) and averaged 0.01 µJ per pulse. Postexposure acuity was measured using high-luminance backgrounds, and the duration of the visual deficit was defined as the total time from exposure to the animal’s return to its preexposure baseline. *Diamonds* represent a single Q-switched pulse, *circles* represent two pulses, and *triangles* represent three pulses.

onstrates the length of time required for full recovery following single, double, and triple Q-switched pulses of different retinal spot diameters. All exposures were below the ED<sub>50</sub> level and were presented on-axis. This figure shows that the length of recovery following a single Q-switched pulse was considerably shorter than that following either a double or triple exposure. For this subject, a single, minimal diameter (<50 µm) Q-switched pulse produced no significant shift in postexposure acuity, and only a minor shift was noted for multiple pulses. As the size of the retinal exposure area increased from 100 µm to >800 µm, not only did the size of the maximum deficit increase, as previously shown in other figures, but also the duration of the visual deficit increased from 5 min to almost 40 min. For all pulse conditions, larger-diameter exposures produced more consistent and sustained deficits than those for small-diameter exposures. The relationship

between the two- and three-pulse conditions was complex, with the two-pulse condition often producing a longer-lasting deficit than the three-pulse condition.

Variations in the energy per pulse had some impact on the nature of the visual deficit, but these differences were only evident for relatively large spot sizes. As previously shown, single Q-switched pulses of minimal spot size (<50 µm) produced little observable change in postexposure acuity even for high-energy exposures at or slightly above the ED<sub>50</sub>. Increasing the area of retinal involvement by increasing the spot size and/or by increasing the number of presented Q-switched pulses, however, did produce immediate, but still transient, changes in the animal’s postexposure acuity.

In Figures 4-14 and 4-15, the recovery functions for relatively large-diameter exposures (500 µm) are shown for two different energy levels, 1.0 µJ (ED<sub>50</sub> for small spot exposures) and 0.1 µJ (1 log unit below the ED<sub>50</sub>), and pulse rates (single and triple pulses). In Figure 4-14, the animal was exposed on two separate sessions to a single Q-switched pulse at both of these energy levels. In Figure 4-15, the same animal under the same exposure conditions was exposed to three, rather than two, Q-switched pulses within a 150-ms time interval at these same two energy levels. All expo-

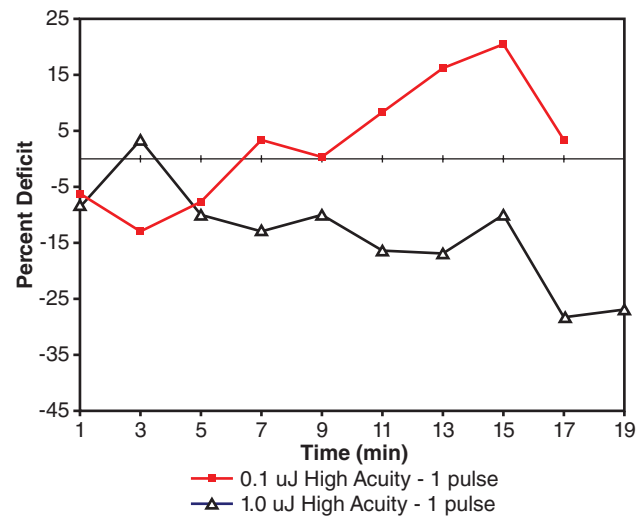


**Figure 4-14.** Single Q-switched pulse exposure at two different exposing energy levels. A single pulse was presented at either 1.0 µJ (*triangles*) or 0.1 µJ (*squares*). Both exposures were made on-axis, and each exposure produced a retinal spot size of 500 µm. Postexposure acuity was measured using high-luminance backgrounds against darkened Landolt rings. Our tracking technique was used to plot postexposure acuity. The *abscissa* represents the minutes following exposure; the *ordinate* represents the animal’s average acuity relative to its preexposure acuity.

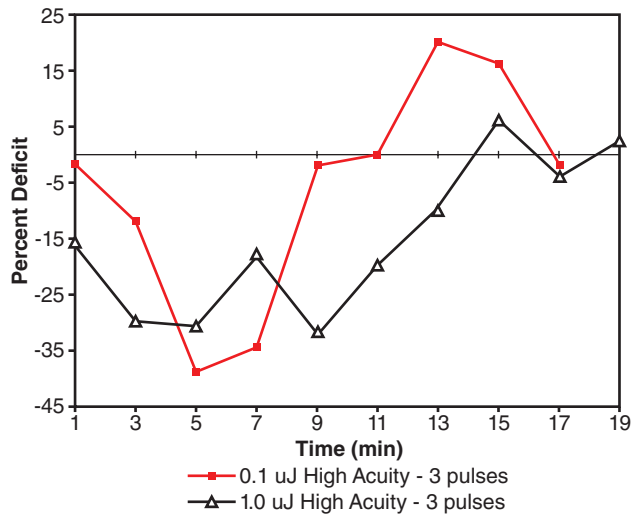


**Figure 4-15.** Three Q-switched pulses at two different energy levels. Three pulses at 1.0  $\mu\text{J}$  (triangles) and 0.1  $\mu\text{J}$  (squares) were presented within a 150-ms window. Both the high- and low-energy exposures were made on-axis; each pulse produced a retinal spot size of 500  $\mu\text{m}$ . Postexposure acuity was measured using high-luminance backgrounds against darkened Landolt rings. Our tracking technique was used to plot postexposure acuity. The *abscissa* represents the minutes following exposure; the *ordinate* represents the animal's average acuity relative to its preexposure acuity.

sure were presented on-axis, and the animal's postexposure acuity was measured using high-luminance targets. When exposed to a single, low-level, Q-switched pulse, the animal's postexposure acuity dropped only slightly for a brief period before quickly returning to its preexposure level within approximately 8 min. This curve (see Figure 4-14) demonstrates little initial impact of this exposure on the ability of the animal to maintain a consistent postexposure threshold comparable to its preexposure level. However, during the later portions of the test session, the animal demonstrated the same type of enhancement in visual performance that had been noted previously for those exposures where an immediate deficit was observed. The initial deficit was  $<15\%$  (with a Snellen acuity of 20/20) and was very transient in nature.

The enhancement in postexposure acuity was somewhat more pronounced and less transient in nature, although by the end of the 20-min postexposure test session, the animal's acuity had returned to its preexposure baseline. At the higher energy level (1.0  $\mu\text{J}$ ), the initial deficit was not remarkable during its early stages, especially compared to previously reported initial deficits; but, with time, the animal demonstrated a gradual, but significant, drop in visual acuity that lasted for the duration of the test session. Within the 20-

min postexposure session, visual acuity had dropped by approximately 25%, and no recovery or enhancement effect was noted. By the next day, the animal's acuity had returned to its preexposure baseline level; and, in the days that followed, no permanent deficit was noted. No additional exposures were presented to this animal for several weeks, and no similar decline in acuity during the later portions of the exposure sessions were noted in this animal when a triple, rather than a single, Q-switched pulse was presented (see Figure 4-15).

Larger, more consistent and prolonged visual deficits were observed for minimal spot diameters of higher energy density when the number of successive pulses presented within an exposure session was increased. Shown in Figure 4-16 are the recovery curves following two different energy exposures presented to the same animal over the course of several different sessions. In Figure 4-16a, four Q-switched pulses were presented within a 200 ms exposure window. Each pulse had an energy density of 0.5  $\mu\text{J}$  and produced a retinal spot diameter of approximately 50  $\mu\text{m}$ . However, given the number of individual pulses presented, the actual size of the exposure site was likely significantly larger due to the animal's involuntary and ongoing voluntary eye movements. The total area of exposure could have varied from 50  $\mu\text{m}$ , assuming total overlap to greater than several hundred microns, and assuming little retinal overlap in individual pulses. The total energy presented was slightly below the  $\text{ED}_{50}$  for this exposure condition. In Figure 4-16a, immediately after exposure, this animal's visual acuity dropped to 35% of its preexposure acuity and remained depressed at this level for approximately 15 min before gradually returning to its preexposure level within 21 min. Increasing the energy density per pulse to 1.0  $\mu\text{J}$  produced a similar recovery function (Figure 4-16b). In this case, however, the animal's preexposure acuity decreased by as much as 25% during the first 15 min after the exposure; within 17 min, the animal's acuity had returned to its preexposure level. In both of these exposures, the animal's long-term acuity remained unaffected even though exposure energy densities were at or near the  $\text{ED}_{50}$ . This animal's baseline acuity was followed for several days after exposure with no additional laser irradiation. Postexposure acuity remained at baseline and was consistent with acuity in the animal's control (unexposed) eye. With higher-energy pulses or with pulses that exposed a greater overall area of the fovea (larger spot diameters), some increased variability in acuity was noted in subsequent test sessions even though the animal's average acuity approximated its preexposure level. Within days, however, these slight

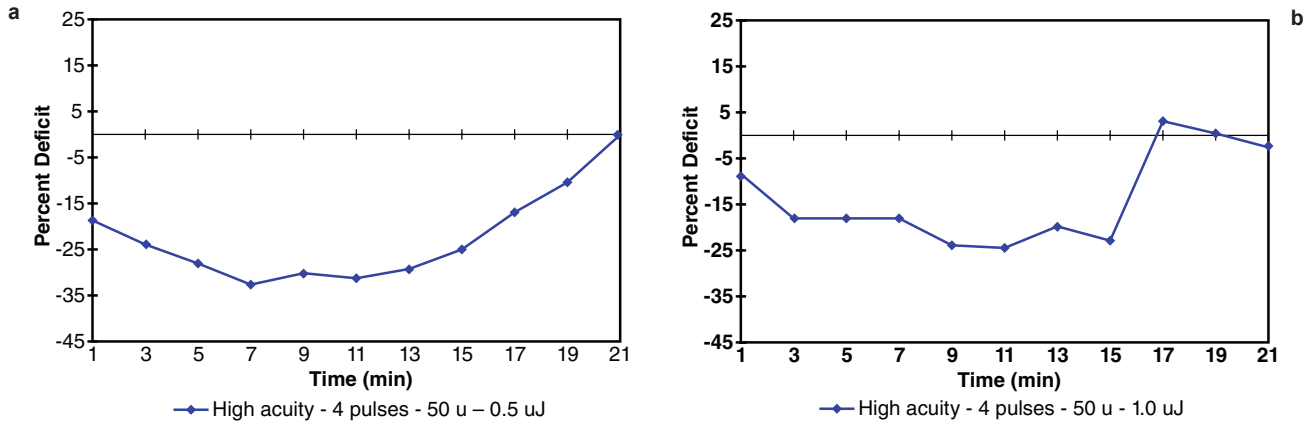


**Figure 4-16.** Multiple (4) Q-switched pulses at two different energy levels. On separate exposure sessions, this animal was exposed to four Q-switched pulses from a Nd:YAG (neodymium-doped yttrium aluminum garnet) laser. All four pulses were presented within a 200-ms exposure window and were presented coaxial with the gap in a threshold Landolt ring (on-axis) producing a 50- $\mu\text{m}$  diameter spot on the retina. The energy density of each pulse was the same, but was (a) 0.5  $\mu\text{J}$  per pulse and (b) 1.0  $\mu\text{J}$  per pulse. Postexposure acuity was measured using high-luminance backgrounds against darkened Landolt rings. The *abscissa* represents the minutes following exposure; the *ordinate* represents the animal's average acuity relative to its preexposure acuity.

variability differences disappeared, and the animal appeared fully recovered from the exposure.

As previously shown, variations in the number of pulses, the energy per pulse, or the area of involvement (spot diameter) produced no significant lingering effects beyond the actual exposure session for those exposures at or below the maximum permissible exposure (MPE). The impact of each exposure appeared independent of previous exposures, and there were considerable similarities in recovery for each exposure in terms of the magnitude of the initial deficit and the time required for full recovery. At the transitional zone between temporary and permanent visual loss, however, the impact that any one exposure had on the recovery from another exposure was dependent on the energy of the exposure, as well as the number and sequence of previous high-energy exposures. As the energy per pulse increased and individual exposures approached the transition zone between temporary and permanent visual loss, there were predictable increases in the time course of recovery functions for successive exposures presented over days or weeks. This cumulative effect on the nature of recovery occurred in spite of the fact that individual exposures were separated from each other by at least 24 h, and recovery from previous exposures often appeared complete within their immediate 30-min postexposure sessions. Typically, in the transition zone, successive exposures produced only slight variations in the size of the initial deficit, but there were significant differences in the time to full recovery for each exposure. In some cases, recovery first appeared complete within 30 to 45 min. However, 24 h later, the animal had more dif-

ficulty maintaining a stable baseline and often showed slight decreases in acuity.

In Figures 4-17 and 4-19, the differential effects of successive exposures are shown for two animals exposed to 50 and 100  $\mu\text{J}$  pulses. Each animal was exposed to only one 15 ns pulse per day. Following the first several exposures at these energy levels, recovery was complete within a matter of minutes. In the case of the 50  $\mu\text{J}$  exposures (see Figure 4-17), for the first three exposures at this energy level, the animal's postexposure acuity returned to its baseline preexposure level within the test session; no prolonged effect beyond the initial transient deficit was noted in subsequent baseline testing over the next several days. The maximum initial deficit elicited by these high-energy, large spot exposures was approximately 70%, and acuity began to improve almost immediately after this unusually large initial acuity shift. Total recovery time for the first exposure was approximately 10 min, for the second exposure 14 min, and for the third exposure 18 min. For the fourth exposure, the size of the initial deficit was similar to the previous three exposures, and the animal's acuity again returned to its baseline within 18 min.

However, unlike the first three exposures, for this fourth exposure the animal was unable to maintain this baseline level, and its acuity again dropped and leveled off at approximately 35% of its preexposure level. Full recovery did not occur within the next 30 min, and this animal's postexposure acuity on subsequent days appeared unusually inconsistent both within- and between-test sessions. This animal received no additional exposures, and its postexposure acuity baseline remained somewhat depressed over the next 6 months.

During this period, the animal failed to consistently maintain a stable baseline in its exposed eye, varying by as much as 50% from the preexposure baseline. The acuity in its unexposed eye was normal and consistent over the course of the next 6 months.

Figure 4-18 shows the actual daily average postexposure acuity for this animal following a fourth single 50  $\mu$ J pulse, with considerable uncharacteristic day-to-day variability. This animal's postexposure acuity to various background targets was also followed over the next several weeks. Overall, the animal's acuity during this 16-day period averaged nearly 25% below its previous consistent baseline, varying some days by as much as 50% from its preexposure level. Several other animals exposed in a similar manner did not show as great a day-to-day variation as seen in this example; instead, their acuity remained more consistently depressed for several days after exposure before any significant recovery occurred. All animals exposed to single 50  $\mu$ J pulses ultimately regained their acuity to a level consistent with both their control eye and their preexposure baseline. Often, however, it took several months before this recovery occurred.

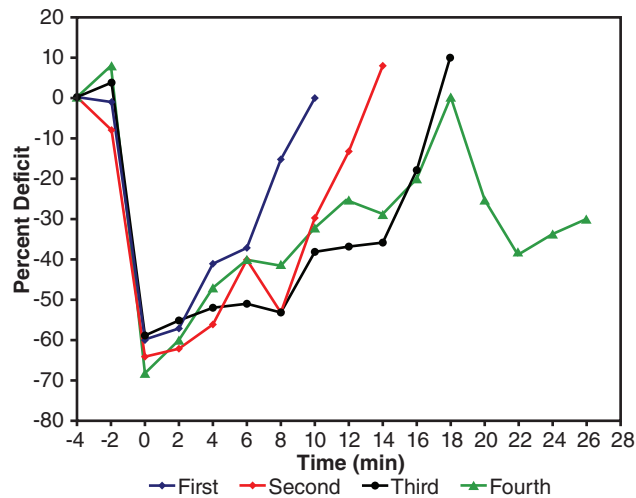


**Figure 4-17.** Changes in visual acuity following four separate 50- $\mu$ J exposures. This animal was exposed over several weeks to single, high-energy, 532-nm, Q-switched pulses from a Nd:YAG (neodymium-doped yttrium aluminum garnet) laser. Each exposure was presented on-axis and created a 250- $\mu$ m diameter spot on the retina. Only one exposure was made per session (day); postexposure acuity was measured using high-luminance backgrounds against darkened Landolt rings. The *abscissa* represents the minutes following exposure; the *ordinate* represents the animal's average acuity relative to its preexposure acuity. *Blue diamonds* represent the animal's postexposure acuity to the first of four laser pulses, *red diamonds* represent the second pulse, *circles* represent the third pulse, and *triangles* represent the fourth pulse.

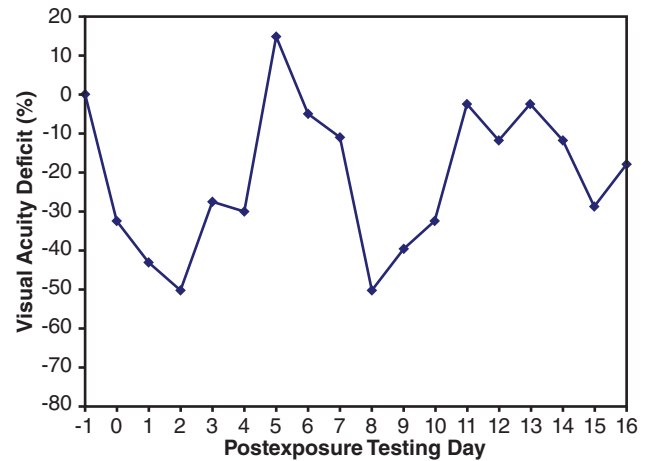


**Figure 4-18.** Mean daily postexposure acuity following multiple 50- $\mu$ J exposures. This animal was exposed to four separate 50- $\mu$ J, 532-nm, Q-switched pulses (see Figure 4-17). Each laser pulse was separated from the other by at least several days. Following each exposure, postexposure testing continued until a stable baseline was again established consistent with this animal's preexposure acuity level. Once a stable baseline was established, the animal was reexposed to another 50- $\mu$ J pulse, and postexposure testing continued until the animal had apparently recovered from that exposure. This figure demonstrates the day-to-day changes in baseline acuity over a 16-day period following the fourth and final 50- $\mu$ J pulse. Each data point represents the average deficit derived from a minimum of 30 to 45 min of testing. No laser exposures were made during this time period. The *abscissa* presents the days after the last exposure; the *ordinate* represents the animal's average postexposure acuity relative to its preexposure acuity.

Similar to the exposure paradigm shown in Figure 4-17, Figure 4-19 demonstrates changes in an animal's immediate postexposure acuity following four separate 100  $\mu$ J pulses. Again, each exposure consisted of a single Q-switched pulse that was positioned coaxial with the gap in a threshold Landolt ring and produced a 250  $\mu$ m spot on the retina. Only one Q-switched pulse was presented per day and only after the animal had established a stable preexposure baseline. In contrast to the exposure paradigm for the 50  $\mu$ J pulse, each 100  $\mu$ J pulse shown in Figure 4-19 was presented at least 5 weeks apart. In the period between exposures, average daily postexposure baselines were measured and are shown in Figure 4-20. At this high-energy level, animals typically had considerable difficulty fully recovering from the exposure during the normal 30-min postexposure session. In Figure 4-19, similar to the recovery functions shown in Figure 4-17, this animal appeared to regain its preexposure acuity baseline for the first three exposures within 15 to 20 min of exposure. But, unlike the recovery to 50  $\mu$ J pulses,

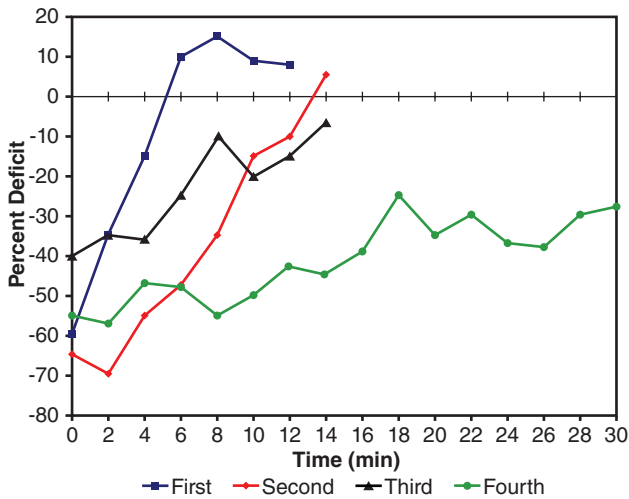


**Figure 4-19.** Changes in visual acuity immediately following each of four separate 100- $\mu$ J exposures. This animal was exposed over a several weeks to high-energy, 532-nm Q-switched pulses from a Nd:YAG (neodymium-doped yttrium aluminum garnet) laser. Each exposure was a single Q-switched pulse presented coaxial with the gap in threshold Landolt ring (on-axis) and created a 250- $\mu$ m diameter spot on the retina. Only one exposure was made per session. Postexposure acuity was measured using high-luminance backgrounds against blackened Landolt rings. Postexposure acuity was plotted against the animal's preexposure baseline for each of the four separate exposures. The *abscissa* represents time after exposure; the *ordinate* represents average postexposure acuity. The recovery function following the first exposure is plotted with *squares*, the second exposure is plotted with *diamonds*, the third exposure is plotted with *triangles*, and the fourth exposure is plotted with *circles*.

this animal exposed to 100  $\mu$ J pulses was unable to maintain its preexposure baseline in subsequent daily postexposure testing in spite of the fact that no additional exposures were made.

Postexposure testing continued for this animal for 5 weeks before each reexposure; this process was repeated five times until eventually the animal failed to recover during the 30-min postexposure session. For example, after the first exposure, the animal appeared to fully recover within 6 min, but in the days that followed demonstrated a subtle but consistent depression in acuity (see Figure 4-20). Several months later, this animal's acuity remained stabilized and depressed at 0.75 (min of arc)<sup>-1</sup>. At this point, the animal was exposed to a second 100  $\mu$ J pulse. Again, its immediate postexposure acuity appeared to return to its previously reduced baseline in approximately 14 min. After 24 h, the animal's baseline acuity level again shifted from 0.75 (min of arc)<sup>-1</sup> to 0.6 (min of arc)<sup>-1</sup>.

This animal's acuity was followed for another 5 weeks before a third exposure was made. The imme-

diated deficit produced by a third exposure was again similar to those of the first two exposures and quickly recovered to its previously depressed baseline in approximately 15 min before dropping to a stable baseline of approximately 0.4 (min of arc)<sup>-1</sup>. After another 5-week period of almost daily testing, the animal was exposed to a fourth 100  $\mu$ J pulse. Following the fourth exposure, the animal was unable to regain its previous stabilized acuity within the 30-min test session. After still another delay of 5 weeks, this animal was exposed to a fifth and final 100  $\mu$ J pulse (not shown). The reaction to this exposure was somewhat similar to that of the fourth exposure in that the animal was unable to regain its immediate preexposure acuity during the 30-min postexposure session and in subsequent testing remained somewhat stable at approximately 0.4 (min of arc)<sup>-1</sup>. These lingering effects for each of the five separate 100  $\mu$ J pulses represent this animal's average postexposure acuity over a 5-month period and demonstrate a growing visual deficit with each 100  $\mu$ J pulse.

Long-term changes in visual acuity were followed in this animal after the fifth and final 100- $\mu$ J, Q-switched pulse. Figure 4-21 shows the gradual improvement change in this animal's acuity over a period of several years. More than 3 years later,

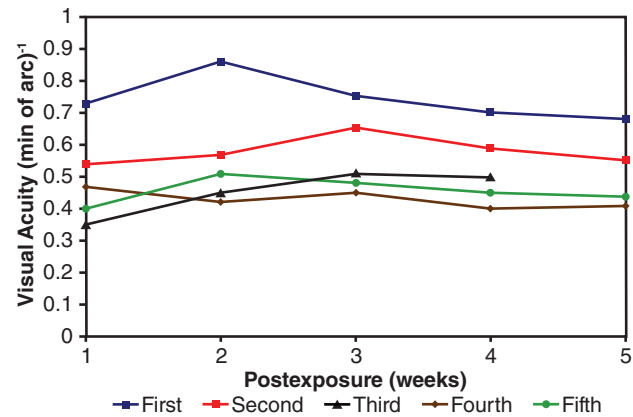


**Figure 4-20.** Mean weekly postexposure acuity following each of five 100- $\mu$ J pulses. Each curve represents the average weekly acuity measured daily over a period of 5 weeks. Visual acuity was derived under high-luminance conditions; no laser exposures were made during each of the 5-week postexposure periods shown. *Blue squares* represent the average postexposure acuity following the first exposure, *red squares* represent the average postexposure acuity following the second exposure, *triangles* represent the average postexposure acuity following the third exposure, *diamonds* represent the average postexposure acuity following the fourth exposure, and *circles* represent the average postexposure acuity following the fifth exposure. Postexposure acuity is plotted on the ordinate in (min of arc)<sup>-1</sup>.

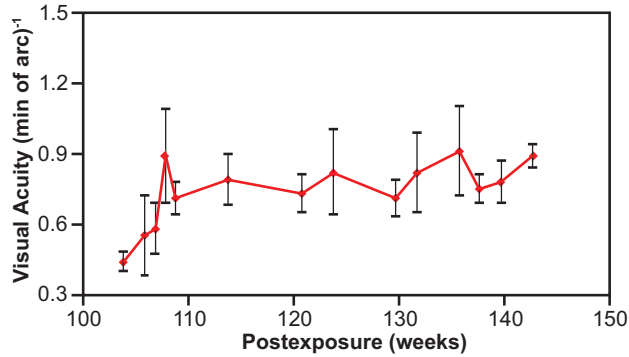


**Figure 4-21.** Long-term postexposure changes following high-energy exposure. Average weekly visual acuity for one animal exposed to five separate 100- $\mu$ J pulses. All exposures were presented on-axis. Each data point (diamonds) represented mean weekly acuity measured in  $(\text{min of arc})^{-1}$  and the vertical bars through each data point represent the range of variability (minimal and maximal) of these test sessions. Visual acuity was measured using high-luminance, achromatic backgrounds against darkened Landolt rings (high-acuity criterion) and plotted on the ordinate in  $(\text{min of arc})^{-1}$ .

this animal's acuity of  $0.9 (\text{min of arc})^{-1}$  was still depressed almost 40% from its original preexposure baseline of  $1.45 (\text{min of arc})^{-1}$ , but was significantly better than the  $0.4 (\text{min of arc})^{-1}$  level noted in the weeks immediately following this final exposure. Acuity in this animal's control eye remained normal and consistent during this entire period of postexposure testing.

Complete spectral acuity curves were also derived for this subject's control and exposed eyes using both high (*photopic*) and low (*scotopic*) luminance conditions. Figure 4-22 represents the spectral acuity curves using a high-acuity criterion. Interestingly, spectral acuity showed less of a maximum deficit than achromatic acuity. Using achromatic targets, this animal's maximum acuity in the exposed eye was  $0.9 (\text{min of arc})^{-1}$  relative to  $1.4 (\text{min of arc})^{-1}$  in the control eye, whereas chromatic acuity in the exposed eye was  $0.8 (\text{min of arc})^{-1}$  versus  $1.1 (\text{min of arc})^{-1}$  in the control eye. For the exposed eye, the shape of its spectral acuity curve, however, was somewhat flat across the entire visible spectrum while in the control eye; and this animal's spectral acuity peaked between 480 and 520 nm. Overall, the two spectral curves for the control and exposed eyes overlapped

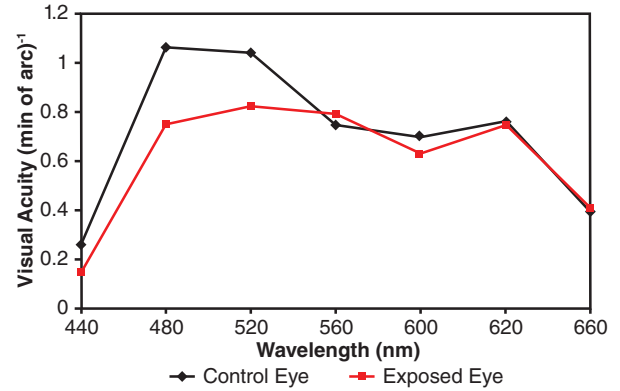


**Figure 4-22.** Postexposure spectral acuity. Postexposure acuity for an animal exposed to five separate 100- $\mu$ J Nd:YAG (neodymium-doped yttrium aluminum garnet) laser pulses that produced long-term deficits in acuity. Acuity was measured using different chromatic backgrounds equated for equal energy against darkened Landolt rings. *Diamonds* represent the spectral acuity of the unexposed (or control) eye (OD; oculus dexter [right eye]); *squares* (OS; oculus sinister [left eye]) represent the exposed eye. Each data point represents the mean acuity for this spectral background tested over a period of approximately 1 month.

considerably, except in the short-wavelength region of the spectrum where the short-wavelength sensitivity in the exposed eye was approximately 30% reduced from that of the unexposed eye. Not shown here are the spectral acuity curves for low-acuity criterion (low-luminance conditions). Under these luminance levels, the spectral curves for the control eye were also flat across most of the visible spectrum and to that extent were similar to the curve shown here for the exposed eye. The spectral curve for the exposed eye under these reduced luminance conditions (low-acuity criterion) was greatly depressed; the criterion was difficult to derive at the spectral extremes, leaving measurements available only for midspectrum background targets.

Fundus examination of exposed eyes was routinely performed and often showed punctate lesions in both the fovea and parafovea in those animals with permanent functional losses. Retinal optical coherence tomography scans in these animals showed retinal thinning and NFL loss in the macula and papillomacular bundle. Fluorescein angiography typically showed leakage at the punctate foveal damage site within the foveal vascular zone.

## DISCUSSION

The visual deficits that were elicited by laser exposure are consistent with what would be expected with temporary or permanent foveal loss. Exposures

presented outside the fovea produced little or no effect on maximum photopic visual acuity. Exposure of wide regions of the fovea or macula by large-diameter

spots or by repetitive, small-diameter pulses led to immediate and often sustained decreases in visual acuity. Typically, the animal's visual acuity dropped immediately after exposure to a maximum deficit that remained depressed for several minutes before gradually returning to its preexposure level. The magnitude of the initial deficit appeared related to the area of retinal involvement, whereas the duration for full recovery was more dependent on the energy rather than the size of the exposure.

Consistent with the nature of our visual task, exposure to single Q-switched pulses of minimal spot diameters produced little or no acuity deficits. Irradiation of very small foveal regions ( $<50\ \mu\text{m}$ ) would not be expected to disrupt enough photoreceptors and/or neural pathways in any one region to seriously limit the processing of incoming visual information. Even for energy densities significantly above the  $ED_{50}$ , multiple pulses presented over several exposure sessions or within the same exposure session would be necessary to produce damage in a large enough region to alter an animal's ongoing photopic acuity. The only exception might be transient changes that could result from exposures powerful enough to induce retinal bleeding and thereby obstruct the light pathway as it travels through the ocular media. At energy levels near the  $ED_{50}$ , both single and multiple Q-switched pulses did temporarily impede the ability of the animal to consistently maintain a baseline photopic acuity, perhaps suggesting changes in the opacity within the eyeball. Although large-diameter exposures and more pulses per exposure produced larger and more sustainable visual deficits, it was only the combination of these factors that elicited a permanent deficit in visual acuity.

A relatively wide range of different retinal spot sizes (50–825  $\mu\text{m}$ ) was used in this study, and these variations in the size of the exposure did produce initial deficits of varying degrees. Typically, the larger the spot size, the greater the initial deficit and, to some extent, the longer the time required for full recovery. The same relationship was generally true for the number of Q-switched pulses. Single, 15 ns pulses normally had only a minimal impact on the ability of the animal to maintain its preexposure baseline unless the spot size was large ( $>200\ \mu\text{m}$ ). These brief laser pulses would allow a highly motivated observer the ability to "look" around the affected regions and still maintain maximum visual performance. Consistency might be a problem, however, and with single Q-switched pulses, we did observe subtle changes in discrimination errors (false positives and misses) and response times that were not characteristic for the subject. This was especially the case when intense, but extremely small, punctate exposures were made within

the fovea. On the one hand, bleeding and involuntary eye movements possibly affected the ability of even highly motivated animals to consistently maintain the discriminanda on functional rather than irradiated or clouded regions of the fovea. On the other hand, multiple Q-switched pulses, even for these small spot sizes, typically elicited more sizable initial deficits that required longer recovery times. Larger diameter multiple pulses produced even larger visual deficits and required still more time for full recovery.

Increasing the power density of individual pulses generally produced longer recovery times and, in some cases, produced prolonged deficits that extended beyond the typical 30-min postexposure test session. Multiple Q-switched pulses at energy levels  $10\times$  below the  $ED_{50}$  produced only transient deficits in immediate postexposure acuity. These deficits were reminiscent of the deficits we observed for long-duration exposures (millisecond time domain) below the  $ED_{50}$  or for Q-switched pulses (nanosecond time domain) above the  $ED_{50}$  where neuropathological effects would be expected. However, if the area of retinal exposure was small (50–100  $\mu\text{m}$ ), due either to the number of pulses presented and/or the diameter of the exposure site, little change was noted either to the animal's immediate or long-term postexposure visual acuity regardless of the exposure energy used. Even for initial exposures at energy levels that were significantly above the  $ED_{50}$  ( $10\times$  to  $100\times$ ), remarkably little decrement in visual acuity was often noted. In several cases, single Q-switched pulses of larger retinal diameter ( $>100\ \mu\text{m}$ ) produced more pronounced visual deficits that were similar in nature to the transient deficits produced by large-diameter, longer duration (either millisecond CW exposures or multiple nanosecond Q-switched) pulses. When significant areas of the fovea were involved, an immediate drop in baseline photopic acuity resulted, and what followed was a gradual recovery that often lasted 45 min or longer. Both the magnitude and duration of the observed visual deficits were related to the amount of retinal area involved (exposure spot size) and to the number of Q-switched pulses presented.

With larger spot sizes, the exposure energy clearly influenced the duration of the initial deficit, as well as the likelihood of full recovery within the remaining time of the test session. The impact of multiple exposures under this condition often became prolonged and sometimes permanent for Q-switched pulses above the  $ED_{50}$ . Unlike millisecond time-domain exposures, no similar cumulative effect was noted for repeated nanosecond time-domain exposures at energy levels significantly below the  $ED_{50}$ . The lack of any corresponding cumulative impact for Q-switched pulses

is noteworthy. Although high-energy exposures often produced transient acuity shifts, our results suggested that for the smallest diameter and shortest duration exposures, the functional criterion may be limited in defining a permanent effect, even when minimal neuropathy may be present. However, we have noted significant initial effects and possibly subtle longer-term changes in discrimination errors, especially when multiple punctate exposures within the fovea are made. These less conspicuous effects could possibly reflect more global dysfunction when briefly presented discriminable targets fall on "altered" retinal regions. The consequences of repeated exposures within these transitional energy zones may be particularly important in understanding these changes. The demonstration of any transitional zone between temporary and permanent functional changes for nanosecond time-domain exposures similar to that found for millisecond time-domain exposures would suggest the possibility of increased susceptibility of exposed tissue to permanent damage, especially in situations involving brief, but repeated, low-level energy exposures.

The transient effects observed in this study at energy levels below the  $ED_{50}$  and below those that might cause edema suggest that single, isolated Q-switched pulses can have a significant impact on an animal's immediate postexposure acuity, even if the consequence is not permanent. The time course of these transient effects suggests reversible receptor or photochemical alterations that may bypass the normal time parameters of visual adaptation. Still unresolved is the possibility that repeated nanosecond time-domain exposures within the same retinal region might ultimately become additive and eventually produce permanent functional changes similar to those that we have demonstrated for millisecond time-domain exposures. If that were the case, over time these transient visual deficits might blossom into significant permanent functional loss with minimal initial warning. Such changes would likely not be immediately apparent through an ophthalmoscope, but might be observable if visual functioning was carefully tracked.

The energy required to produce a threshold functional deficit for the nonhuman retina in the millisecond time domain (CW exposures) approximated damage thresholds using morphological criteria; and, in some cases, especially when using repeated exposures or large spot sizes, was somewhat lower than that found using nonfunctional criteria.<sup>29,30</sup> Pathology thresholds for nanosecond time-domain exposures are even lower than for millisecond time-domain exposures and may be the result of higher peak powers produced by these briefer pulses.<sup>31</sup> Such concentrations of energy can create, in addition to a

thermal component, acoustic damage when they interact with the retina. In comparison to longer-duration exposures, this acoustic or mechanical insult may be sufficient to rupture tissue membranes at much lower energy levels than is possible in the millisecond time domain. In relation to the function of retinal tissue, Q-switched pulses are deposited within the neural layers of the retina before photoreceptors are normally able to respond. These rapid deliveries of light energy could temporarily short circuit the full response of the photoreceptor system and bypass its normal adaptation function. However, because the pulse is still sufficient to cause morphological damage, alterations in permanent visual function might still occur. Due to its limited temporal and spatial domains, repeated nanosecond exposures may be required to influence large enough areas necessary to produce a significant overall functional effect.

Using exposures in the millisecond time domain, we have shown that regardless of the size of the spot on the retina, even larger areas of involvement typically occur because of the smearing effect of involuntary eye movements. Somewhat independent of the differences in exposure energies used, the immediate and often transient acuity deficits that resulted from millisecond time-domain exposures were larger than those shown here using nanosecond time-domain exposures. Given the differences in spatial characteristics of these two types of exposures, repeated exposures over different sessions would more likely irradiate the same retinal regions when large-diameter, longer-duration (millisecond time domain) exposures are used. With minimal diameter Q-switched pulses of limited spatial extent, repeated exposures in either the same or different exposure sessions would have a much lower likelihood of exposing the same retinal region. Thus, the lack of any cumulative impact observed when using Q-switched pulses at energy densities below the  $ED_{50}$  for nanosecond time-domain exposures, but not for the millisecond time-domain exposures, could be explained on the basis of nonoverlapping sites and not strictly by differences in the delivery of energy over time.

In our previous studies using millisecond time-domain exposures, permanent acuity deficits were noted following repetitive exposures at energies below the MPE.<sup>24</sup> Recent ophthalmoscopy on one animal suggests that these types of cumulative functional deficits, even at levels below the MPE, can be associated with distinct pathology in the eye. Although in the current study, no similar cumulative functional effect was noted for low-energy, Q-switched pulses, a distinct cumulative effect was evident for small spot exposures at energy densities above the MPE. Similar to lower-energy and longer time-domain exposures,

repetitive high-energy Q-switched pulses produced longer and longer recovery times until evidentially a permanent functional deficit was observed. Unlike the millisecond time-domain exposures, however, the size of the initial deficit with repeated exposures did not significantly change when high-energy nanosecond time-domain exposures were made. This suggests that even small-diameter, high-energy, Q-switched pulses can produce a significant dazzle effect independent of any permanent change that it might produce.

These results may be consistent with other functional studies using slightly different exposure conditions. For example, it has been demonstrated that repeated extended source exposures slightly above the MPE for a single-extended source exposure induce a bull's-eye maculopathy that imaged confocally; these results suggested a primary or secondary retinal nerve fiber defect. However, in this case, no permanent loss in high-contrast grating acuity was observed.<sup>32</sup> Visual targets in that study did not exceed a Snellen acuity of 20/40, whereas in our studies animals normally achieved preexposure photopic acuity levels better than 20/15 when using Landolt ring targets. The defi-

cits noted in our studies are above the maximum acuity range previously noted.

Of particular interest in our results was the consistent temporary enhancement in acuity (hyperacuity) that followed each acuity deficit produced by low-energy, Q-switched exposures. Hyperacuity was routinely observed following either single or multiple 0.1  $\mu$ J, Q-switched pulses and, like the preceding acuity deficit, this enhancement was also not sustainable. The cause of this hyperacuity is difficult to discern, but it might be significant that it was only obvious with on-axis exposures and with low-energy exposures that produced small and transient deficits. A similar enhancement effect might not be expected in off-axis exposures where neural networking and spacing between cells are different. Exposing the fovea to intense light might eventually disinhibit the areas within and around the central fovea by fatiguing the retina's lateral inhibition mechanisms. The sensitivities and recovery times for this neural inhibitory mechanism and that of the photochemical process in the receptor cell could be different and could possibly account for this apparent enhancement.<sup>33</sup>

## SUMMARY

In conclusion, several hypotheses were made and empirically supported. First, light-induced damage to the retina disrupts visual performance, as well as retinal physiology. The type and magnitude of the functional alteration appear related to the location and degree of the retinal insult. Structural damage to photoreceptors should affect an organism's fine-resolution capability through changes in the organism's inherent color, brightness, and contrast sensitivities. These changes should be especially distinct if foveal areas are involved. Damage to areas outside the fovea may disrupt scotopic and peripheral vision, but would not be easily detected unless more complex visual field testing is performed. Using our performance paradigm, only foveal damage would disrupt photopic acuity, although scattered damage throughout the parafoveal region should increase within-session variability. Typically, we have defined these parafoveal and peripheral exposures as misses; in reality, the animal's retina was likely exposed, but not in the region where photopic acuity would be altered. This notion is supported by the limited acuity changes produced when our exposures were purposely made off-axis from the animal's fixation point.

Second, the size of the irradiated retinal area should directly influence the magnitude of the observed visual deficit. As previously stated, irradiation of very small regions of the fovea still permits a highly motivated

observer to develop alternative viewing strategies that could effectively allow him/her to look around isolated dysfunctional regions and maintain a high-acuity criterion. Larger spot sizes or multiple exposures within the same region would make this strategy less effective. Also, exposing larger retinal zones increases the probability of a "successful" foveal exposure because a larger retinal region is irradiated, which increases the probability that at least some portion of the central fovea will be involved. Exposing the animal to a single pulse (nanosecond duration) of a relatively small spot diameter (<100  $\mu$ m) evokes only a small lesion even at the highest power densities and therefore elicits only minimal acuity shifts that might appear transient in nature. Edema, bleeding, and other damage and repair mechanisms are often delayed, and their impact would not be immediately obvious.

Somewhat unexpected was the lack of consistent and large-scale deficits when relatively large-diameter (100–500  $\mu$ m), single Q-switched pulses were presented. These very brief exposures produced only small observable deficits for both high- and low-acuity criterion. It is likely, however, that exposures of this brief duration (15 ns) did not allow for involuntary eye movements to produce enough "smearing" of the exposure and therefore increased the probability that the exposure site was not consistently centered within the fovea. Hence, below the ED<sub>50</sub>, our paradigm

appeared unable to fully delineate transient acuity deficits in spite of the fact that some temporary or even semipermanent damage might have occurred. Using more spatially complex targets or more sensitive measures of contrast sensitivity and/or color vision could delineate subtle functional changes not observed in the current study. Repetitive Q-switched pulses were shown to summate their individual effects and create significant transient shifts in immediate postexposure acuity, even for those energy levels significantly below the MPE. Fewer, larger-diameter exposures should produce the same overall effect as would longer-duration, single exposures from a CW laser. Furthermore, repeated low-energy exposures within the same retinal region, even if delayed by hours or days, may increase the long-term susceptibility of that particular tissue to insult. If the nature of nanosecond exposures is consistent with that observed for millisecond exposures, these individual exposures can be presented beyond the time needed for full functional recovery to any one exposure. In both nanosecond and millisecond exposures, we have noted within the transitional zone that repetitive exposures that initially produce only minimal baseline shifts can increase the variability of the animal's postexposure acuity. This more erratic behavior was normally temporary, lasting only several days or weeks, and might be the result of ongoing repair mechanisms within the affected tissue. With time, variability should decrease and acuity improve as the repair mechanisms proceed, as surrounding unaltered photoreceptors migrate into the area now devoid of active photoreceptors, and/or as the animal learns to compensate by improving its fixation ability to stabilize the critical features of the target on unaltered portions of the retina.

Shifts in postexposure acuity noted in our study could also be explained by an initial edema within or surrounding the exposed tissue. Swelling of the retina tissue would alter photoreceptor orientation, spacing, and possibly neural functioning. These changes could clearly alter the ability of the exposed animal to resolve spatial detail. If swelling occurred, the initial acuity deficit would be expected to grow in time, stabilize, and possibly then decrease depending on the time course of the edema. Combined with ocular clouding, due to even minor hemorrhages that could develop from low-energy exposures, transient acuity deficits could also have resulted from increased light scatter that created a blurred image within an otherwise intact neural encoding system. As the hemorrhage dissipated over time, acuity would have then returned to normal.

These optical changes in image clarity should be more transient than those caused by encoding problems associated with photoreceptor repair.

Even more immediate and transient postexposure acuity changes could be explained by a dazzle effect. Its time course could correspond to the normal regeneration of pigments or could be prolonged depending on any reversible actinic insult that might also accompany the exposure. Psychological variables associated with even temporary blindness might also adversely impact the organism's normal viewing and decision-making strategies. Changes in the ratio of false alarms to correct detection and misses to correct rejections might signal shifts in the organism's confidence level and strategies used to complete the task. Ultimately, however, in forced-choice tasks where there is a high payoff for positive performance, observers should develop strategies to maximize their perceived rewards. Following laser exposure, such strategies should involve altered points of fixation to maximize the use of retinal regions with the highest ongoing sensitivities. Our data clearly support the notion that our animals did engage in defensive behavior that maximized their existing visual sensitivities because their visual acuity did not drop to zero after exposure, but rather quickly stabilized at new levels consistent with the resolution power of the parafovea.

Research to address ocular damage in the workplace should extend beyond the problem of treatment intervention to include training strategies for alternative viewing of critical target features. Studies of this type provide unique opportunities to generate immediate postexposure visual performance under a wide array of exposure conditions both below and above the  $ED_{50}$ . There is potential value in the opportunity to train personnel to minimize the impact of potentially damaging light through strategies that support continuation of visually guided missions. These strategies are important not only for those with pathology, but also for those who might be only temporarily disabled by laser irradiation. Data from studies of this kind could also be used to further delineate the impact of dazzle, changes in the integration of neural retinal circuits, minute enzyme changes within irradiated tissue, and changes in ocular opacity that might not otherwise be evident by traditional ophthalmoscopic examination. We would not expect that these data would be inconsistent with the morphological data, but they may reveal more subtle effects—including photochemical and neural processes—that could equally degrade visual performance.

### Acknowledgments

This research was supported in part by a contract to Ohio Wesleyan University from the US Army Medical Research Detachment, Walter Reed Army Institute of Research, Brooks Air Force Base, Texas.

The death of Dr Harry Zwick was a tremendous personal and professional loss. Dr Zwick's lifelong dedication to advancing our understanding of the visual system and his commitment to his research program and fellow researchers were without parallel.

In conducting the research described in this chapter, the investigators adhered to the *Guide for the Care and Use of Laboratory Animals*, as promulgated by the Committee on Revision of the Guide for Laboratory Animal Facilities and Care, the Institute of Laboratory Animal Resources, and the National Academy of Sciences–National Research Council.

### REFERENCES

1. Curcio CA, Sloan KR Jr, Packer O, Hendrickson AE, Kalina RE. Distribution of cones in human and monkey retina: individual variability and radial asymmetry. *Science*. 1987;236:579–582.
2. Roorda A, Metha AB, Lennie P, Williams DR. Packing arrangement of the three cone classes in primate retina. *Vision Res*. 2001;41:1291–1306.
3. Ham WT Jr, Geeraets WJ, Mueller HA, Williams RC, Clarke AM, Cleary SF. Retinal burn thresholds for the helium-neon laser in the rhesus monkey. *Arch Ophthalmol*. 1970;84:797–809.
4. Powell JO, Bresnick GH, Yanoff M, Frisch GD, Chester JE. Ocular effects of argon laser radiation. II. Histopathology of chorioretinal lesions. *Am J Ophthalmol*. 1971;71:1267–1276.
5. Robbins DO, Zwick H. Changes in spectral acuity following brief laser (647 nm) exposure. In: Vierriest G, ed. *Colour Vision Deficiencies V*. Bristol, England: Adam Hilger Press, Ltd.; 1980: Chap 2.
6. Zwick H, Bedell RB, Bloom KB. Spectral and visual deficits associated with laser irradiation. *Mod Probl Ophthalmol*. 1974;13:299–306.
7. Zwick H. Visual functional changes associated with low-level light effects. *Health Phys*. 1989;56:657–663.
8. Tso MOM. Photoc maculopathy in rhesus monkey. A light and electron microscopic study. *Invest Ophthalmol*. 1973;12:17–37.
9. Custis PH, Gagliano DA, Zwick H, Schuschereba ST, Regillo CD. Macular hole surgery following accidental laser injury with a military range finder. *Proc SPIE*. 1996;2674:166–174.
10. Stuck BE, Zwick H, Molchany JW, Lund DJ, Gagliano DA. Accidental human laser retinal injuries from military laser systems. *Proc SPIE*. 1996;2674:7–20.
11. Marshall J. Structural aspects of laser-induced damage and their functional implications. *Health Phys*. 1989;56:617–624.
12. Marshall J. Blinding laser weapons. *Br Med J*. 1997;315(7120):1392.
13. Zwick H, Ness JW, Molchany JM, Stuck BE, Loveday J. Utilization of scanning laser ophthalmoscopy in laser induced human retinal nerve fiber layer damage. *Proc SPIE*. 1998;3246:144–147.
14. Zwick H, Stuck BE, Dunlap W, Scales DK, Lund DJ, Ness JW. Accidental bilateral Q-switched neodymium laser exposure: treatment and recovery of visual function. *Proc SPIE*. 1998;3254:80–89.

15. Zwick H, Ness JW, Molchany JM, Stuck BE, Loveday J. Neural motor ocular strategies associated with the development of a pseudofovea following laser-induced macular damage and artificial macular occlusion: is the fovea replaceable? *J Laser Appl.* 1998;10:144–147.
16. Zwick H, Stuck BE, Scales DK, Brown J, Ness J. Longitudinal evaluation of selected human laser eye accident cases. *Proc SPIE.* 2001;4246.
17. Ramon Y, Cajal S. *Degeneration and Regeneration of the Nervous System.* May RM, trans. New York, NY: Haffner Publishing Co; 1928. Vol 2.
18. Houle JD. Demonstration of the potential for chronically injured neurons to regenerate axons into intraspinal peripheral nerve grafts. *Exp Neurol.* 1991;113:1–9.
19. Tom VJ, Steinmetz MP, Miller JH, Doller CM, Silver J. Studies on the development and behavior of the dystrophic growth cone, the hallmark of regeneration failure, in an in vitro model of the glial scar and after spinal cord injury. *J Neurosci.* 2004;24:6531–6539.
20. Brittis PA, Silver J. Multiple factors govern intraretinal axon guidance: a time-lapse study. *Mol Cell Neurosci.* 1995;6:413–432.
21. Inman DM, Steward O. Ascending sensory, but not other long-tract axons, regenerate into the connective tissue matrix that forms at the site of a spinal cord injury in mice. *J Comp Neurol.* 2003;462:431–449.
22. Marshall J, Hamilton AM, Bird AC. Histopathology of ruby and argon laser lesions in monkey and human retina. A comparative study. *Br J Ophthalmol.* 1975;59:610–630.
23. Robbins DO, Zwick H, Bearden BD, Evans BS, Stuck BE. Visual acuity changes in rhesus following low level Q-switched exposures. *Proc SPIE.* 1997;2974:94–104.
24. Robbins DO, Zwick H. Subthreshold functional additivity occurring at the transition zone between temporary and permanent laser-induced visual loss. *Proc SPIE.* 1996;2674:44–52.
25. Pizzorusso T, Medini P, Berardi N, Chierzi S, Fawcett JW, Maffei L. Reactivation of ocular dominance plasticity in the adult visual cortex. *Science.* 2002;298:1248–1251.
26. Robbins DO, Zwick H, Holst GC. Functional assessment of laser exposures in awake, task-oriented, rhesus monkeys. *Mod Probl Ophthalmol.* 1974;13:284–290.
27. Robbins DO, Zwick H, Holst GC. A method for producing foveal retinal lesions. *Behav Res Meth Instr.* 1973;5:457–461.
28. Robbins DO, Zwick H, Leedy M, Stearns G. Acute restraint device for rhesus monkeys. *Lab Animal Sci.* 1986;36:68–70.
29. Robbins DO. *Analysis of Retinal Function Following Laser Irradiation.* Fort Detrick, MD: US Army Medical Research and Development Command; 1992. Final Report Contract DAMD17-83-C-3172 and DAMD17-88-C-8032.
30. Zwick H, Robbins DO, Stuck BE, et al. Small-spot laser exposure effects on visual function. *Proc Int Soc Opt Eng.* 1990;1207:71–88.
31. Zwick H, Robbins DO, Reynolds SB, et al. Effects of small spot foveal exposure on spatial vision and ERG spectral sensitivity. In: Drum B, Moreland JD, Serra A, ed. *Color Vision Deficiencies X.* Dordrecht, The Netherlands: Kluwer Academic Publishers; 1991: 581–597.
32. Rhodes JW, Zuclich JA, Zwick H, et al. Bullseye-gap maculopathy associated with repeated large spots, Q-switched laser exposure. Paper presented at: Annual Meeting of the Association for Research in Vision and Ophthalmology; May 1–6, 1994; Sarasota, FL.
33. Zwick H, Gagliano DA, Zuclich JA, Stuck BE, Lund DJ, Glickman RD. Confocal scanning laser evaluation of repeated Q-switched laser exposure and possible retinal NFL damage. *Proc SPIE.* 1995;2391:634–639.